https://doi.org/10.5194/egusphere-2026-2098
Preprint. Discussion started: 8 May 2026

Volcanic sulfur dioxide total columns and layer height from the IASI and TROPOMI Layer Height products: preprocessing and assimilation on a 0.1° regional domain of MOCAGE

Mickaël Bacles [1] and Vincent Guidard [1]

[1]Météo-France, CNRS, Univ. Toulouse, CNRM, Toulouse, France

Correspondence: Mickaël Bacles (mickael.bacles@meteo.fr)

Abstract. Sulfur dioxide (SO_2) emitted by volcanic activity constitutes an important hazard for aircraft operations. Volcanic Ash Advisory Centres (VAACs) rely on satellite observations to monitor and on the assimilation of these observations to predict the evolution of volcanic plumes. TROPOMI (Tropospheric Monitoring Instrument) observations are already operational in the MOCAGE (Modèle de Chimie Atmosphérique à Grande Échelle) model. However, in this MOCAGE configuration, SO_2 plumes are assumed to be located between 3 and 10 km of altitude. Recent developments aim to improve SO_2 modelling by taking into account plume altitude data provided by the TROPOMI Layer Height (TROPOMI LH) product and the Infrared Atmospheric Sounding Interferometer (IASI) in the assimilation. Before being assimilated, these observations are preprocessed according to two methods depending on the assimilated instrument.

This approach is evaluated for two contrasting eruptions: the explosive eruption of Mount Etna on 4 August 2024 and the low-altitude eruption on the Reykjanes Peninsula between 22 and 25 August 2024. Independent observations from the Ozone Mapping and Profiler Suite (OMPS) and AirBase surface measurements are used for validation. The results show that the use of plume altitude improves the vertical representation of SO_2 and facilitates the detection of high SO_2 total columns. Despite the limited availability of altitude observations, their use improves plume structure and transport consistency.

1 Introduction

SO_2 emitted by volcanoes is hazardous to aviation. Not only can it damage aircraft engines (Prata, 2009), but it can also pose a threat to the health of passengers when concentrations are high (Schmidt et al., 2014).

To ensure aviation safety, Volcanic Ash Advisory Centres (VAACs) use many satellite instruments to observe the location and intensity of SO_2 plumes. These instruments include TROPOMI, which retrieves SO_2 total columns from ultraviolet (UV) radiances, and IASI, which provides observations of total columns from infrared (IR) radiances. However, these instruments do not directly provide information on the future evolution of the plumes. Incorporating these observations into chemistry transport models (CTMs) enhances the accuracy of volcanic plume simulations. The assimilation of obsevations from GOME-2 (Global Ozone Monitoring Experiment-2) and OMI (Ozone Monitoring Instrument) into the Integrated Forecasting System for atmospheric composition (IFS-COMPO) (Flemming and Inness, 2013), or with the joint assimilation of TROPOMI and IASI

https://doi.org/10.5194/egusphere-2026-2098
Preprint. Discussion started: 8 May 2026

into MOCAGE (Bacles et al., 2025) has shown improvements in plume forecasts. Nevertheless, in these studies, assumptions regarding plume altitude are prescribed during the assimilation process.

The vertical distribution of volcanic SO_2 is one of the main sources of uncertainty in modelling and predicting volcanic plumes. Although satellite instruments provide reliable measurements of total SO_2 columns, the injection altitude of the SO_2 plume remains a key factor controlling its transport, chemical transformation, and atmospheric lifetime, and therefore strongly influences the accuracy of the plume forecasts. Due to vertical wind shear and variations in atmospheric stability with altitude, even a moderate error in plume height can lead to significant deviations in the simulated trajectory and spatial extent, several hours to several days after emission. In many eruptions, the volcanic ash plume and the SO_2 plume are spatially and vertically co-located, as observed during the Eyjafjallajökull eruption in 2010 (Sears et al., 2013). However, when ash and SO_2 plumes are released at different altitudes, the ash and SO2 plumes no longer coincide spatially. A striking example is the Grímsvötn eruption in 2011, when ash and SO_2 plumes were observed at different altitudes and transported in different directions due to contrasting winds at different heights (Prata et al., 2017).

Taking into account plume altitude during assimilation has already shown a significant improvement for the case of Raikoke in 2019 in the IFS COMPO system, where the TROPOMI Layer Height product was assimilated (Inness et al., 2022). Nevertheless, several limitations remain. First, altitude diagnostics from the TROPOMI layer height product are only available when the total column exceeds 20 DU, limiting their use to the most concentrated parts of the plume. In addition, suspicious altitudes are frequently diagnosed at the edge of the plume, where a mixture of clear air and SO_2 plume can bias the retrieval and lead to artificially lower heights. In order to limit the impact of these artefacts on assimilation, a specific pre-processing algorithm was developed in our study to identify and exclude these unrepresentative altitudes.

Although the consideration of plume heights in data assimilation has recently been evaluated in global systems, its impact at the regional scale remains poorly documented. However, a regional domain offers several advantages for studying volcanic plumes, such as finer spatial resolution, which allows for better representation of concentration gradients and narrow plume structures. Nevertheless, observations from some instruments, such as IASI, can cover multiple meshgrids of the model, and each observations can be separated by several model meshgrids. To assimilate such observations across the regional domain, a preprocessing algorithm is developed. In this paper, we develop two preprocessing algorithms to assimilate TROPOMI LH and IASI observations at the regional scale before examining the impact of altitude-constrained assimilation. Two contrasting eruptions are studied: the eruption of Mount Etna on 4 August 2024, which injected SO_2 into the upper troposphere (Hastings and Sennert, 2024) and for which IASI and TROPOMI LH observations are available, and the eruption on the Reykjanes Peninsula between 22 and 25 August 2024, for which only TROPOMI LH observations are available and which showed a plume close to the surface (Sennert, 2024). For the Mount Etna eruption, IASI and TROPOMI LH are first assimilated separately and then jointly. The analysis outputs are compared against independent OMPS observations and compared with the operational MOCAGE assimilation system, which currently assimilates TROPOMI total columns. For the eruption on the Reykjanes Peninsula, simulated surface SO_2 concentrations are compared with AirBase measurements.

The remainder of this paper is organised as follows. Section 2 presents the case studies. Section 3 describes the observations. Section 4 introduces MOCAGE CTM and its assimilation system. Section 5 presents the assimilation configurations, including

https://doi.org/10.5194/egusphere-2026-2098
Preprint. Discussion started: 8 May 2026

the operational setup and the new altitude-constrained configuration. Section 6 describes the preprocessing algorithms applied to the IASI and TROPOMI LH observations. Sections 7 and 8 present the results for the Etna and Reykjanes eruptions, respectively.

2 Description of case studies

2.1 Mount Etna eruption on 4 August 2024

Mount Etna is a volcano located in Sicily (37.748°N, 14.999°E) that erupts regularly. In this study, we focus on the eruption that began on 4 August 2024 at 04:08 UTC and ended on 4 August 2024 at 13:18 UTC, with a significant decrease in volcanic activity from 09:10 UTC. According to Hastings and Sennert (2024), this eruption released a large amount of ash and SO_2, with the main plume reaching an altitude of approximately 10 km above sea level (a.s.l). A second plume was detected at 6.2 km a.s.l. Both plumes moved toward the south east. During the most active phase of the eruption, the number of planes landing at Catania airport was reduced to six per hour due to volcanic activity. Under normal circumstances, the number of landings per hour reaches up to 18 per hour.

2.2 Eruption on the Reykjanes Peninsula from 22 to 26 August 2024

The end of 2023 marked the beginning of a period of intense activity on the Reykjanes Peninsula in south-western Iceland. According to Sennert (2024), seven eruptive episodes occurred between December 2023 and December 2024. In this study, we focus on the eruption that began on 22 August 2024 at 21:26 UTC and ended on 26 August 2024. The most active volcanic activity was observed during the first 24 hours. At the onset of the eruption, the SO_2 and ash plume reached an altitude of 1 km above ground level and drifted southeastward. By 24 August, the SO_2 plume reached Scotland.

3 Description of the instruments

3.1 TROPOMI

TROPOMI, on board the polar-orbiting Sentinel 5 Precursor (S5P) satellite, provides information on air quality and climate (Reshi et al., 2024) with a high spatial resolution of 5.5 x 3.5 km at the nadir. TROPOMI is a hyperspectral radiometer allowing measurements of radiances on spectral bands extending from the ultraviolet (UV) to the shortwave infrared (SWIR) domains. Every day, it measures radiance spectra at a local time of 13:35 UTC (Veefkind et al., 2012) which constitute the level 1 product. Due to the wavelengths, there are no observations during night.

Level 1 products are converted into SO_2 total columns in near-real-time thanks to the differential optical absorption spectroscopy (DOAS) algorithm operated by the Royal Belgian Institute for Space Aeronomy (BIRA) and the German Aerospace Center (Deutsches Zentrum für Luft- und Raumfahrt, DLR) (Theys et al., 2017). First, slant column densities (SCDs), cor-

https://doi.org/10.5194/egusphere-2026-2098
Preprint. Discussion started: 8 May 2026

responding to the integrated SO_2 concentration along the mean atmospheric optical path, are computed. From these SCDs, SO_2 total columns are retrieved for four scenarios corresponding to the use of different prior SO_2 vertical profiles. The first one, provided by a forecast made by the TM5 chemical transport model (Huijnen et al., 2010), is used in the case of polluted scenarios. The second profile, which aims to represent the well-mixed anthropogenic or volcanic sulphur dioxide conditions, is a box extending from ground level to 1 km of altitude. Two other profiles are intended to represent SO_2 emitted by effusive eruptions in the upper troposphere and by explosive eruptions above the lower stratosphere. These two profiles are a box of 1 km thickness, respectively, centred at 7 and 15 km high. For each scenario, air mass factors (AMF) and averaging kernels (AVKs) are computed.

TROPOMI provides some information on the quality of the retrievals with a value for each pixel ranging from 0 for uncertain retrieval to 1 for the best retrieval. It is recommended to use only observations where this value is greater than 0.5. Moreover, TROPOMI enables observations to be classified into four distinct categories described in Table 1. TROPOMI data are available in the Copernicus Data Space Ecosystem (https://dataspace.copernicus.eu/, last access: 21 January 2026).

Flag value	Description
0	No detection
1	Enhanced SO_2 detection
2	Enhanced SO_2 detection in vicinity of known volcano (300 km of a volcano)
3	Enhanced SO_2 in vicinity of anthropogenic source (100 km of an anthropogenic source)
4	Enhanced SO_2 in SAA or for SZA $> 70°$

Table 1. Detection flags provided for the TROPOMI SO_2 product. In this table SAA is South Atlantic Anomaly and SZA is solar zenith angle.

3.2 TROPOMI Layer Height

Hedelt et al. (2019) have developed a product, called TROPOMI Layer Height (TROPOMI LH), which allows to have information on the altitude of a SO_2 plume. A first step consists of simulating many reflectance spectra for wavelengths ranging from 310 to 335 nm with the LInearized Discrete Ordinate Radiative Transfer (LIDORT) model (Spurr et al., 2008) by varying values of the solar zenith angle (SZA), viewing zenith angle (VZA), relative azimuth angle (RAA), O_3 and SO_2 vertical column density, layer height, surface albedo, and surface pressure. The TROPOMI spectral response function, defining the instrument's sensitivity as a function of wavelength, is applied to the previous reflectance spectra. The simulated reflectance spectra are separated into 10 principal components (PCs). These PCs and auxiliary data (surface information, SZA, VZA, RAA and O_3 total columns) are used as input of the Full-Physics Inverse Learning Machine (FP_ILM) algorithm. This machine learning algorithm allows to diagnose the SO_2 height with an accuracy of 2 km and its corresponding total column.

https://doi.org/10.5194/egusphere-2026-2098
Preprint. Discussion started: 8 May 2026

This product provides information on retrieval quality thanks to a value ranging from 0 for uncertain retrieval to 1 for best retrieval. It is recommended to use only observations where this value is greater than 0.5. In addition to the quality of the retrieval, information on the specific conditions affecting the retrieval is given by a number whose meaning is described in Table 2. In the case where a pixel is affected by several specific conditions, this number is summed. It is recommended to use observations if this number is less than 16, but the diagnosed height of the plume can be affected by the presence of aerosols absorbing and sulfate aerosols. TROPOMI LH data are available in the Copernicus Data Space Ecosystem (https://dataspace.copernicus.eu/, last access: 21 January 2026).

Value	Description of the flags
0	Successful layer height retrieval
1	Input feature range exceeded
2	Layer height exceeds 30 km of altitude
4	Aerosol index > 2. Presence of absorbing aerosols
8	Aerosols index < 0. Presence of sulfate aerosols
16	Retrieved VCD below training range
32	Retrieved layer height is below zero
64	Layer height retrieval was not triggered
128	Input data missing

Table 2. Pixel flags provided by the TROPOMI LH product and their corresponding meanings.

3.3 IASI

IASI is a spectrometer measuring thermal infrared radiances in the spectral range of 645 cm^{-1} to 2760 cm^{-1} with a resolution of 0.5 cm^{-1}. This instrument is onboard both MetOp-B and MetOp-C satellites. The IASI instrument observes the atmosphere globally twice a day at approximately 09:30 and around 21:30 local time (Clerbaux et al., 2009) and acquires measurements over a swath width of 2200 km, using 30 arrays of four elliptical pixels. The size of the pixels varies from 12 × 12 km at the nadir to approximately 40 × 20 km at the swath edges, due to the increasing viewing angle.

IASI is particularly well-suited to monitor a wide range of atmospheric trace gases, including carbon monoxide (CO, George et al. (2009)), ammonia (NH_3, Clarisse et al. (2009)), volcanic SO_2 (Clarisse et al., 2008) or volcanic hydrogen sulfide (H_2S, Clarisse et al. (2011)). For SO_2, radiance measurements are converted into total column amounts using the ULB-LATMOS retrieval algorithm (Clarisse et al., 2012). This algorithm enables the retrieval of SO_2 total columns ranging from 0.5 to 5000 DU, with low uncertainties. Additionally, a dedicated algorithm developed by Clarisse et al. (2014) allows the retrieval of SO_2 plume altitude with an uncertainty of approximately 0.5 km, as well as the associated column. IASI data are publicly available at the AERIS data centre (https://iasi.aeris-data.fr/, last access: 21 January 2026).

https://doi.org/10.5194/egusphere-2026-2098
Preprint. Discussion started: 8 May 2026

3.4 OMPS

OMPS is a nadir-viewing spectrometer operating in the ultraviolet spectral range. This sensor is onboard the Suomi National Polar-orbiting Partnership (SNPP) and NOAA-20 polar-orbiting satellites. The Nadir Mapper, component of OMPS, measures earthshine radiances and solar irradiance for wavelengths between 300 nm and 420 nm with a spectral resolution of approximately 1 nm and a cross-track width of 2800 km. It provides observations once a day at a local Equator-crossing time of approximately 13:30 LT (Li et al., 2024).

In our study, MOCAGE SO_2 total columns are compared with independent observations. For validation we use SO_2 total columns from the OMPS instrument on the NOAA-20 satellite, which has a nadir spatial resolution of 17 km x 13 km. These total columns are retrieved using an algorithm based on a principal component analysis (PCA) method (Li et al., 2017). Vertical columns are computed by assuming a plume altitude of 3 km for the eruption on the Reykjanes Peninsula and 8 km for the eruption of Mount Etna. SO_2 total columns provide by NOAA-20 satellite can be downloaded from the NASA Earthdata website (https://omps.gesdisc.eosdis.nasa.gov/data/NOAA20_OMPS_Level2/OMPS_N20_NMSO2_PCA_L2_Step1.1/, last access: 29 January 2026).

3.5 SEVIRI Ash RGB product

The Spinning Enhanced Visible and Infrared Imager (SEVIRI) is a radiometer aboard the Meteosat Second Generation (MSG) satellite. It measures radiances across 12 spectral bands, ranging from visible to thermal infrared, covering Europe, the Atlantic Ocean, and Africa. SEVIRI provides observations every 15 minutes at a spatial resolution of 3 km at nadir. More details about SEVIRI are available on the EUMETSAT website (https://www.eumetsat.int/msg-services; last accessed on 12 February 2026).

Due to the multiple spectral bands available on the SEVIRI instrument, several specialised products have been developed that allow the detection of snow (De Wildt et al., 2007), dust (Ashpole and Washington, 2012), severe storms (Bedka, 2011), or volcanic ash and SO_2 plumes (Prata and Kerkmann, 2007). A product known as Ash RGB uses a combination of radiance measurements at three specific wavelengths to show the location of volcanic plumes in near real time. This product employs the 10.8 μm brightness temperature, which is sensitive to warm surfaces and warm clouds, the brightness temperature difference between 12 μm and 10.8 μm , used to detect thin volcanic ash and the brightness temperature difference between 10.8 μm and 8.7 μm to identify water clouds and SO_2 gas plumes. In the Ash RGB product, SO_2 plumes appear in green. More details are available on the EUMETRAIN website (https://eumetrain.org; last accessed on 12 February 2026).

3.6 AirBase network

The AirBase network contains a large number of stations and covers Europe. These stations measure surface concentrations of O_3, SO_2, CO, NO, NO_2, PM_{10}, and $PM_{2.5}$. The metadata associated with the observations describe both the type of station and the environmental conditions under which the measurements are performed. Stations were classified by type as traffic,

https://doi.org/10.5194/egusphere-2026-2098
Preprint. Discussion started: 8 May 2026

industrial, or background, and by location as urban, suburban, or rural. Observations are available on the EEA web application (https://eeadmz1-downloads-webapp.azurewebsites.net/, last access: 29 January 2026).

4 The CTM MOCAGE

MOCAGE is the chemistry transport model developed at Météo-France to simulate atmospheric composition on both global and regional up to four days in advance (Josse et al., 2004). It relies on a semi-Lagrangian transport formulation and can operate using nested configurations with different spatial resolutions. In this study, a regional configuration with a horizontal resolution of 0.1° is used to represent volcanic plume transport over Europe and surrounding regions. In our study, the September 2024 version of MOCAGE is used. For the case of Mount Etna eruption, the regional domain of MOCAGE is forced by chemical boundary conditions of the IFS-COMPO system, operated by the European Center for Medium-Range Weather Forecasts (ECMWF). For the case of Icelandic eruption, the regional domain is forced by MOCAGE on a 0.5° global domain. The vertical grid has 60 hybrid σ pressure levels distributed between the surface and 0.1 hPa, with seven levels in the planetary boundary layer, 20 in the free troposphere and 33 in the stratosphere.

Some meteorological fields, such as wind speed and direction, temperature, humidity, pressure, rain, and clouds, are required because MOCAGE is an offline model. These fields are provided by different numerical weather prediction (NWP) models, Action de Recherche Petite Echelle Grande Echelle (ARPEGE) (Courtier, 1991; Bouyssel et al., 2022) for the global domain and by IFS.

Chemical transformations are represented using the RACMOBUS chemical scheme, which combines two mechanisms. The first, RACM, is used for tropospheric chemistry (Stockwell et al., 1997) and includes the sulfur cycle (Feinberg et al., 2019), while the second, REPROBUS, is dedicated to stratospheric chemical processes (Lefevre et al., 1994). Every 15 minutes, MOCAGE computes the atmospheric composition of 112 gaseous species through 379 chemical reactions and 57 photolysis reactions.

In this study, both primary aerosols, including desert dust, sea salt, black carbon, and organic carbon, and secondary inorganic aerosols, represented by sulfate, nitrate, and ammonium, are modelled (Guth et al., 2016; Sič et al., 2015). The aerosol size distribution is described using a sectional approach with six size bins, defined by the following diameters: 0.002–0.01, 0.01–0.1, 0.1–1.1, 1.1–2.5, 2.5–10 and 10–50 μm. Emissions of desert dust and sea salt depend on wind speed and surface characteristics.

To simulate atmospheric composition, the model incorporates inventories of gaseous and aerosol emissions. Anthropogenic emissions are taken from the MACCity inventory (Lamarque et al., 2010), while biogenic emissions are provided by the MEGAN inventory (Sindelarova et al., 2014). Daily biomass burning emissions, provided by the Global Fire Assimilation System (GFAS; (Kaiser et al., 2012)), are injected into the model at different vertical levels depending on the latitude of the

https://doi.org/10.5194/egusphere-2026-2098
Preprint. Discussion started: 8 May 2026

fires (Cussac et al., 2020). Specifically, biomass burning emissions are released at altitudes of 1 km in the tropics, 2 km at mid-latitudes, and 6 km at high latitudes. All other species, except nitrogen oxides produced by lightning (Price et al., 1997), aircraft emissions (Lamarque et al., 2010) and volcanic sulfur dioxide emitted by passive degassing (Lamotte et al., 2021), are released within the first five levels of the model, which corresponds to approximately 500 m above the surface. Volcanic sulfur dioxide from passive degassing is emitted at the summit of the volcano and at 50 m above the volcano top.

5 MOCAGE data assimilation system

Many species can be assimilated in MOCAGE. This is the case of total ozone columns (Emili et al., 2014) and radiances (Coopmann et al., 2026; Vittorioso et al., 2024; El Aabaribaoune et al., 2021) that allow the improvement of ozone in MOCAGE, as well as the aerosols optical depth (AOD) (El Amraoui et al., 2022), and lidar observations (Cornut et al., 2023) that allow the improvement of aerosol modelling.

The assimilation framework applied in this work is based on a three-dimensional variational (3D-VAR) approach. This method combines short-term model forecasts with observations to estimate the most probable atmospheric state. The correction applied to the model depends on both observation and model error statistics. The analysis increment $\delta x^a = x^a - x^b$ is obtained by minimizing the cost J:

$$J(\delta x) = \frac{1}{2}(\delta x)^T \mathbf{B}^{-1}(\delta x) + \frac{1}{2}(y - \mathcal{H}[x^b] - \mathbf{H}[\delta x])^T \mathbf{R}^{-1}(y - \mathcal{H}[x^b] - \mathbf{H}[\delta x]) \quad (1)$$

In equation 1, $\mathcal{H}$ is the observation operator that allows us to convert the model data into the observation space, and $\mathbf{H}$ is the tangent linear operator of $\mathcal{H}$. Before an assimilation experiment is performed, a complete specification of the $\mathbf{B}$ and $\mathbf{R}$ matrices is required. The background error covariance $\mathbf{B}$ is spatially spread by using a correlation matrix, described in El Amraoui et al. (2020), including both horizontal and vertical components.

The horizontal correlation $C^h_{m,n}$ between two points m and n is defined as follows:

$$C^h_{m,n} = exp[\frac{-d^2}{2({L_x}^2 + {L_y}^2)}] \quad (2)$$

In equation 2, d is the distance between the points m and n, L_x and L_y are the longitude and latitude length scales in kilometres.

In equation 2:

$$L_x = L_y = 2R_e.sin(\frac{\alpha\pi}{360}) \quad (3)$$

https://doi.org/10.5194/egusphere-2026-2098
Preprint. Discussion started: 8 May 2026

with R_e the Earth's radius (6371.22 km) and α is the horizontal length scales. In this study, different length scale values are tested for the assimilation of IASI and TROPOMI LH. Only results for a 0.15° horizontal length scale are shown.

The vertical correlation $C^v_{i,j}$ between two pressure levels (p_i and p_j) is defined as follows:

$$C^v_{i,j} = exp[-100.[log(\frac{p_i}{p_j})]^2] \quad (4)$$

In our study, the vertical correlation value between two consecutive levels is set to 0.5.

5.1 Baseline assimilation of TROPOMI volcanic SO_2 in MOCAGE

In this MOCAGE configuration, volcanic SO_2 total columns retrieved from TROPOMI are assimilated following the methodology described in Bacles et al. (2025), with parameter settings adapted to the present study.

Only observations with a quality flag greater than 0.5, a detection flag of 1, 2 or 3, and an associated slant column larger than 1 DU are assimilated. In the regional domain considered, volcanic eruptions are generally effusive. Consequently, TROPOMI retrievals are used based on the a priori SO_2 profile with maximum at 7 km of altitude.

The averaging kernels are taken into account in the observation operator to represent the vertical sensitivity of the TROPOMI instruments. They are computed following the approach of Theys (2018) and adapted to the 7 km a priori profile as follows:

$$\text{AVK(z)} = \frac{\text{AVK}_{TM5}(z) \times \text{AMF}_{\text{TM5}}(z)}{\text{AMF}_{\text{7km}}} \quad (5)$$

where AVK(z) is the averaging kernel at a given altitude, $\text{AVK}_{\text{TM5}}(z)$ and $\text{AMF}_{\text{TM5}}(z)$ are, respectively, the averaging kernels and the air mass factor at altitude z of the TM5 CTM and AMF_{7km} is the air mass factor for the a priori profile containing a peak at 7 km of altitude.

The observation error standard deviation is taken directly from the uncertainties provided by the TROPOMI instrument (Fig. 1a). The observation error covariance matrix **R** is assumed to be diagonal, implying that observation errors are not correlated.

To vertically constrain the injection of SO_2 during assimilation, a background error standard deviation profile was defined with strong values (1 x 10^{-8} ppv) between vertical levels 49 and 38, which correspond approximately to altitudes between 3 and 10 km. These altitudes are generally representative of volcanic eruptions that occur in the regional domain used for the study. Nevertheless, the altitudes of the plume can be outside this altitude range, as shown in Figure 2. In this figure, assimilation using the configuration described above allows the SO_2 concentration in the grey area to be corrected. However, the plume is outside this range for TROPOMI LH in the case of the eruption on the Reykjanes Peninsula and for TROPOMI LH and IASI in the case of the Mount Etna eruption.

https://doi.org/10.5194/egusphere-2026-2098
Preprint. Discussion started: 8 May 2026

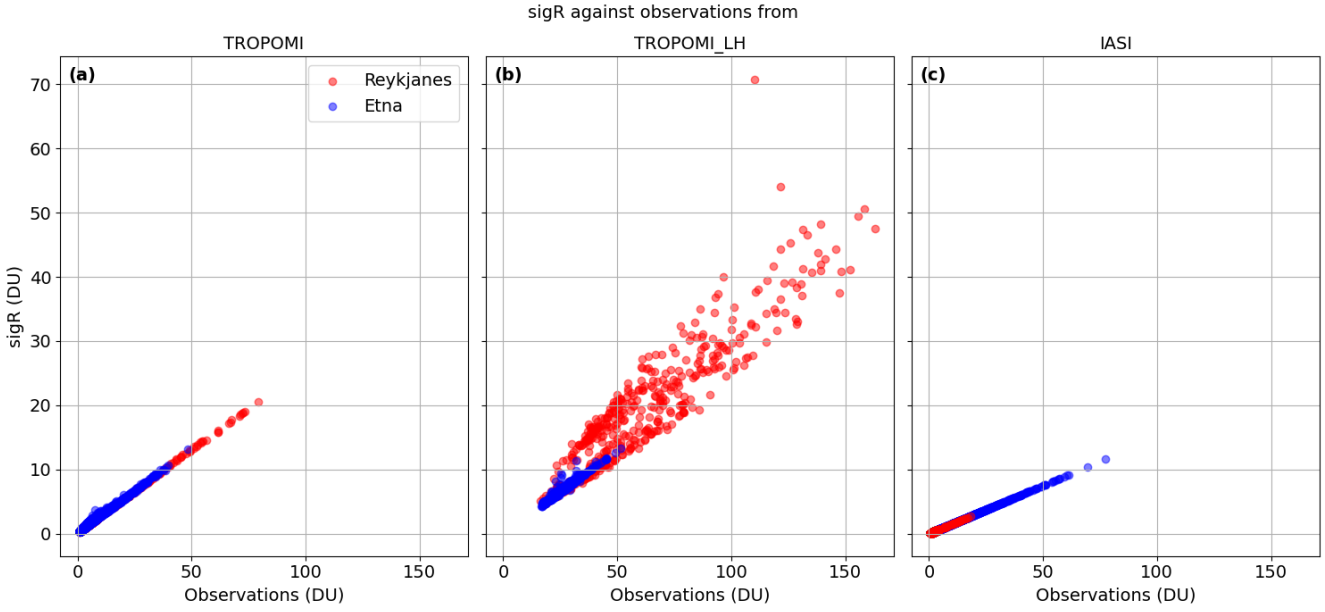

Figure 1. Values of the observation error standard deviation (sigR) according to TROPOMI (a), TROPOMI Layer Height (b) and IASI observations. Blue and red dots represent observations during the Mount Etna eruption and the Sundhnukagigar eruption.

5.2 Data assimilation setup for TROPOMI layer height and IASI instruments

In this configuration, it is assumed that the SO_2 plume is confined between two altitude levels centred on the plume heights provided by the instruments, rather than being distributed from the surface to the top of the atmosphere. A fixed plume thickness of 2 km is adopted, consistent with the uncertainties of the TROPOMI Layer Height product and already used in the IFS-COMPO system (Inness et al., 2022). The altitudes of the centre of the plume that are assimilated are plotted in Figure 2.

Only observations of TROPOMI_LH above 20 DU are taken into account. These observations are assimilated only if the quality flag is greater than 0.5 and the layer height flag is strictly lower than 16. For IASI instruments, only observations above 0.5 DU are assimilated, corresponding to the lowest columns measurable by the instruments. Moreover, observations are assimilated only if the retrieval altitude is higher than 0 km.

In this study, we assume that there is no spatial correlation in the observation error. For TROPOMI, the observation error standard deviation (sigR) is set according to the uncertainties provided by the instrument for each observation (Fig. 1b). The value of the observation error standard deviation ranges from 20 to 70 % of the observations value. For IASI, we set the observation error standard deviation to 15% (Fig. 1c), which is consistent with the uncertainties of the observations (Clarisse et al., 2012).

https://doi.org/10.5194/egusphere-2026-2098
Preprint. Discussion started: 8 May 2026

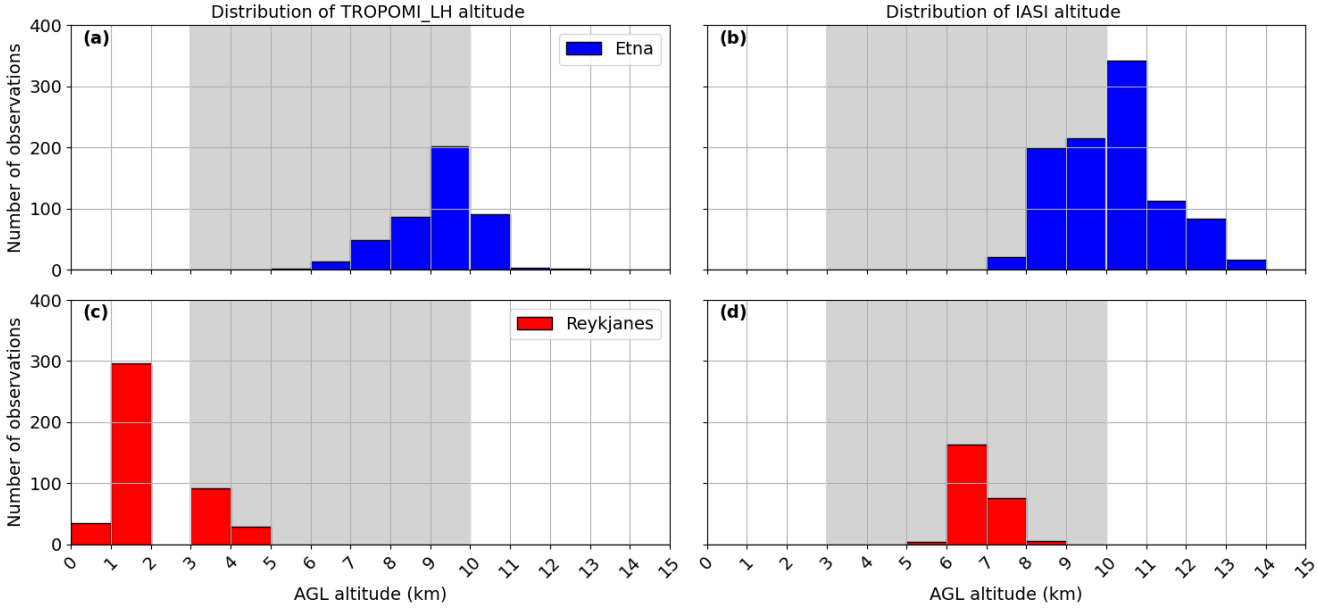

Figure 2. Altitudes of the centre of the plume from TROPOMI_LH retrievals on the first column and from IASI observations on the second one. Blue bars are for the Mount Etna eruption and red bars are for the eruption on Reykjanes peninsula. The light grey area represents the altitudes at which SO_2 is adjusted in the baseline assimilation experiment.

A constant background error standard deviation profile is prescribed, with values of 5 x 10^{-8} ppv. Several tests are performed using different values for the horizontal correlation part of the **B** matrix. The experiments carried out in this study are listed in Table 3.

Experiment	Assimilated observations	Assimilation setup
ref	TROPOMI	Described in 5.1
tropomi_lh_assim	TROPOMI LH	Described in 5.2
iasi_assim	IASI	
joint_assim	TROPOMI LH and IASI	

Table 3. List of experiments carried out in this study.

https://doi.org/10.5194/egusphere-2026-2098
Preprint. Discussion started: 8 May 2026

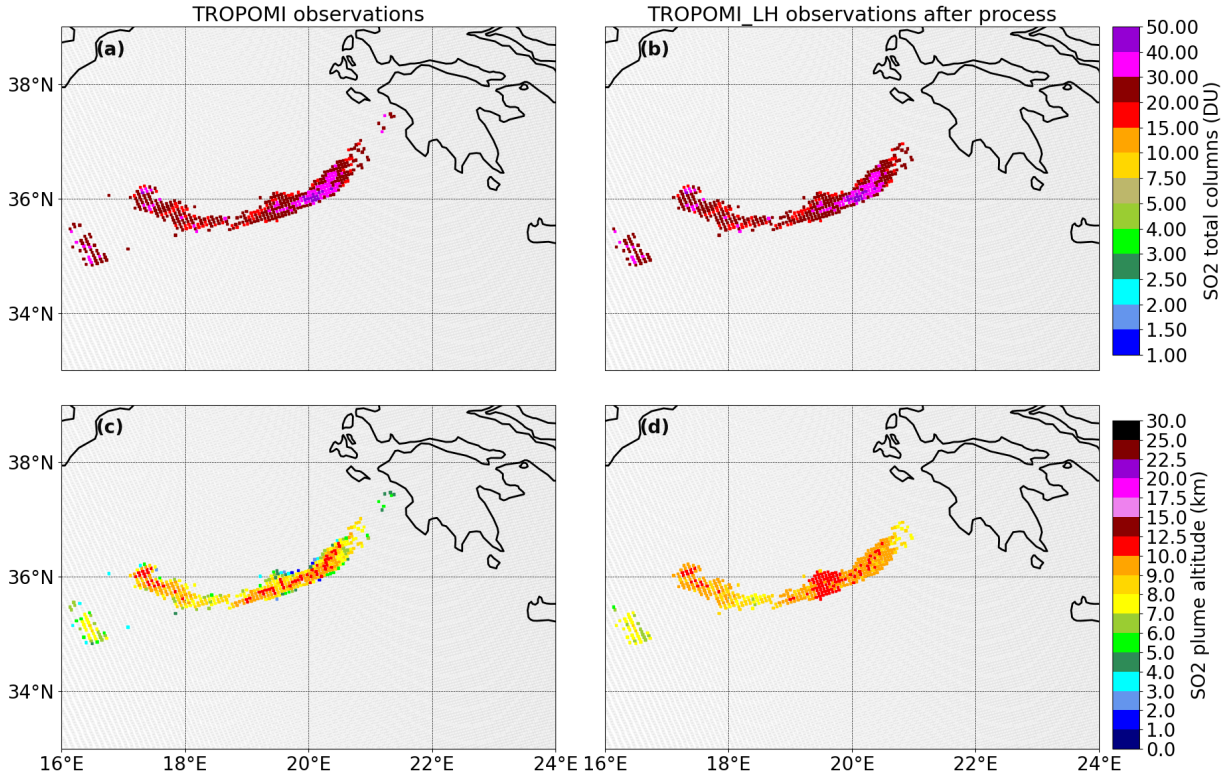

Figure 3. Observed SO_2 total columns (a and b) and associated altitudes (c and d) before (a and c) and after (b and d) applying the algorithm.

6 Preprocess of the assimilated observations

6.1 TROPOMI

For TROPOMI observations, despite the use of quality indicators, the plume altitudes observed at the edge of the plume can differ significantly from those observed at its centre. This discrepancy can be attributed to the partial mixing of clear air and plume, resulting in effective altitudes that are not representative of the main vertical structure of the plume. This behaviour is illustrated in Figure 3c, where lower plume altitudes, sometimes below 3 km, are observed at the edges of the plume. Assimilating these observations can lead to incorrect plume altitude representation in the model.

To avoid assimilating observations with unreliable altitudes, an altitude-based filtering algorithm has been implemented. Figure 4 illustrates the operation of this algorithm for the model grid cell (x, y) located between 35.8°N–35.9°N and 19.3°E–19.4°E.

https://doi.org/10.5194/egusphere-2026-2098
Preprint. Discussion started: 8 May 2026

The algorithm proceeds as follows:

1. **Initial mean calculation:** The mean altitude is first calculated using observations within a window of the 5 × 5 meshgrid centred on the target meshgrid (x, y) if there are at least 10 observations. If this is not the case, observations of the target grid cell are not assimilated. In Figure 4 (a), the observations used for this calculation are shown in blue by crosses or dots when they are located in the target meshgrid (x, y). Observations not used are shown in grey.

2. **Iterative filtering:** A new mean altitude is then calculated, excluding any observations with altitudes greater than 2 km below the current mean value. This process is repeated until the mean altitude converges or until a maximum of 10 iterations is reached. Figure 4 (b) shows the evolution of the mean altitude as a function of the number of iterations, along with the observations used in each calculation. Observations included in the mean calculation are shown in blue (crosses and dots), while excluded observations are shown in red (crossed and dots when they are in the target meshgrid (x, y))). Figure 4 (c) displays the final set of observations used or excluded in the last iteration.

3. **Final altitude assignment:** If the altitudes of the observations in the target mesh grid (x, y) are excluded in the final iteration (red dots in Figure 4 c), their altitudes are set to the last calculated mean altitude. Observations in the target meshgrid (blue dots in figure 4 c) that are retained are assimilated without any altitude modification.

Other grid cell window sizes and minimum observation thresholds within the window have also been tested but are not used because of the presence of low altitudes at the edge of the plume or the loss of information.

Figure 3 displays the TROPOMI LH observations before (a, c) and after (b, d) application of the previously described algorithm. The algorithm removes several isolated observations near Greece and increases the plume altitude, particularly around 19°E/36°N and at the plume edges. The resulting plume altitudes are consistent with IASI observations. In the following, the observations shown in Figures 3 b and d are assimilated.

6.2 IASI

The resolution of the IASI pixel is variable. At the nadir, the pixels are a circle of 12 km in diameter, whereas at the edge of the swath, the pixels are an ellipse of around 40x20 km. Nevertheless, MOCAGE has a horizontal resolution of 0.1° (approximately 10 km). Consequently, some IASI pixels cover several MOCAGE meshgrids. This behaviour is shown in Figure 5 representing the IASI pixels on the MOCAGE grid on 4 August 2024 at 20 UTC. This plot also shows some pixels can be separated by several meshgrids, in particular, when the viewing angle increases. The assimilation of these observations without treatment leads to an underestimation of the SO_2 total columns of MOCAGE.

Two approaches are possible to assimilate these observations. The first consists of applying a large horizontal correlation value in the algorithm process. However, this approach would lead to a volcanic plume too large in size in the model. The second approach, selected in this study, consists in interpolating both SO_2 total columns and altitude plume observations on

https://doi.org/10.5194/egusphere-2026-2098
Preprint. Discussion started: 8 May 2026

the MOCAGE grid.

To align IASI observations with the finer resolution of our model grid, we applied two distinct interpolation methods, selected based on the nature of the retrieved parameters. To illustrate the methodology, we present observations from IASI B on 4 August 2024 at 20:00 UTC, plotted in Figures 6a and c. In these plots, the SO_2 plume is represented by coloured pixels, while grey pixels indicate observations where SO_2 total columns and the associated altitudes are zero.

For SO_2 total columns, we used linear interpolation to ensure a physically consistent spatial transition between adjacent pixels. However, due to the presence of null observations at the plume edges, the interpolated SO_2 total columns tend to be underestimated in these regions. To mitigate this effect, we removed all interpolated observations with values weaker than 0.5 DU, corresponding to the lowest SO_2 total column measuring by IASI. The resulting interpolated SO_2 total columns are plotted in Figure 6b, and their values remain consistent with the initial observations.

For altitude observations, we applied a nearest-neighbour interpolation. This method was selected to avoid artificially low altitudes at the plume edges, which could arise from linear interpolation between high-altitude plume pixels and surrounding null altitude values. All interpolated observations with null altitude are removed. The interpolated altitude plume is presented in Figure 6d.

7 Case study: Mount Etna eruption on 4 August 2024

7.1 Impact on SO_2 and sulfate aerosols

Figure 7 shows the SO_2 total columns fields following the Mount Etna eruption on 4 August at 09:00, 12:00 and 19:00 UTC and on 5 August 2024 at 12:00 UTC The first four rows represent the model simulations: the assimilation of TROPOMI, the assimilation of TROPOMI LH, the assimilation of IASI and the joint assimilation IASI and TROPOMI LH. The last four rows display the corresponding satellite observations from TROPOMI LH, TROPOMI, IASI, and OMPS.

On 4 August at 9:00 UTC, no SO_2 plume is simulated in the ref and tropomi_lh_assim experiments because there is no overpass of the Sentinel-5P satellite since the beginning of the eruption. The simulated SO_2 plume is due to passive degassing, which is included in MOCAGE. The assimilation of IASI leads to the simulation of a SO_2 plume which is consistent with IASI observations.

At 12:00 UTC, a plume is present in all assimilation experiments. The intensity of this plume is underestimated in the ref experiment compared to TROPOMI, TROPOMI LH and OMPS observations. Even if fewer observations are assimilated in tropomi_lh_assim experiment, the spatial extent of the plume is consistent with TROPOMI observations but appears overly extended compared to TROPOMI LH and OMPS observations. In the iasi_assim experiment, the SO_2 total columns remain underestimated, and the plume spreads toward Greece whereas it is over the Mediterranean Sea in the experiment where the

https://doi.org/10.5194/egusphere-2026-2098
Preprint. Discussion started: 8 May 2026

TROPOMI instrument is assimilated. The joint assimilation leads to a plume with strong SO_2 total columns compared to TROPOMI and OMPS observations. Moreover, the plume is more spread compared to the experiments in which TROPOMI LH and IASI observations are assimilated.

At 19:00 UTC, the plume in the ref experiment is inconsistent with IASI observations in both shape and intensity. The simulated plume remains located over Greece, whereas IASI observations show the plume extending over the Mediterranean Sea and Turkey. The plume is more spread in the tropomi_lh_assim experiment but does not reach the same extent as the plume observed by the IASI instruments. When IASI observations are assimilated, the shape and intensity of the plume become consistent with IASI data. The plume is larger and more intense by assimilating both IASI and TROPOMI observations.

On 5 August at 12:00 UTC, the ref simulation agrees better with TROPOMI observations, as TROPOMI data were assimilated between 11:00 and 12:00 UTC. In the TROPOMI LH assimilation experiment, the plume structure remains consistent with TROPOMI observations, 24 hours after the assimilation of the last observations. Nevertheless, it is spatially too spread and the SO_2 total columns values are still underestimated. The spatial extend of the plume are consistent in the iasi_assim and joint_assim experiments and are more spread than the plume observed by TROPOMI instrument. However, the intensity of the plume become closer to the strength of the plume observed by TROPOMI.

Differences in the shape of the plume between the assimilation of each instrument are mainly due to differences in retrieval altitude. Figure 8 shows vertical cross sections at 36.55°N on 4 August at 09:00, 12:00, 18:00 and 19:00 UTC for the simulation in which TROPOMI, TROPOMI LH, IASI, and both IASI and TROPOMI LH are assimilated. The last row of the plot displays the plume altitudes between 35.45°N and 35.65°N observed with IASI in blue and TROPOMI LH in red.

The assimilation of IASI leads to the simulation of a SO_2 plume located between 7 and 15 km of altitude at 9:00 UTC. At the same time, IASI observations detect a plume between 10 and 14 km of altitude. At 12:00 UTC, the simulation that assimilates IASI data shows a plume located between 10 and 14 km of altitude. The modelled plume is higher than that observed by TROPOMI LH, which is located between 7 and 11 km altitude. Due to this altitude discrepancy, the plume in the simulation assimilating TROPOMI LH data is located between 5 and 12 km of altitude. In the joint assimilation experiment, the plume is vertically more extended with a plume located between 5 and 14 km of altitude. In the ref experiment, the assimilation of TROPOMI leads to a simulated plume between 3 and 10 km of altitude around 20°E and 15°E. The simulated concentrations are weaker in this simulation compared to those where altitudes are explicitly considered. The plume simulated around 15°E is not reproduced in the simulation assimilating TROPOMI LH, as the observations do not reach 20 DU. At 18:00 UTC, high concentrations are simulated around 25°E at an altitude of approximately 10 km when IASI data are assimilated. In the other experiments, the plume is more spread out, both vertically and horizontally. The assimilation of TROPOMI LH results in the highest simulated SO_2 concentrations. Simulations assimilating the TROPOMI LH and both IASI and TROPOMI LH instruments yield similar results. The assimilation of TROPOMI produces the lowest concentrations, but the plume structure remains consistent with the experiment assimilating TROPOMI LH.

https://doi.org/10.5194/egusphere-2026-2098
Preprint. Discussion started: 8 May 2026

In MOCAGE, sulfate total columns slightly decrease compared to the reference experiment, particularly in the experiment with the assimilation of IASI, which results in a higher plume altitude. However, this decrease is too slight to observe significant variations in terms of aerosol optical depth (AOD).

7.2 Comparison to independent observations

At 19:00 UTC, the assimilation of IASI observations results in a more vertically extended plume structure around 25°E in the simulation in which this instrument is assimilated. This structure is also present in the joint_assimilation experiment. Nevertheless, this plume is more spread out in this experiment because of the influence of the previous TROPOMI LH assimilation. TROPOMI and TROPOMI LH observations are not available at this time. However, a plume is modelled between 22°E and 26°E, with an altitude of 5 to 10 km. The SO_2 concentrations remain the lowest in the experiment assimilating data from TROPOMI instrument.

In Figure 9 (bottom panel), SO_2 plume exhibits different shapes at 18:00 UTC, depending on the assimilated instrument. The assimilation of IASI data results in a plume that is more widespread toward Turkey, whereas no SO_2 plume is simulated over Turkey when TROPOMI is assimilated. At 18:00 UTC, the MSG ash product (Figure 9, top panel), displays the SO_2 plume in green, encircled in red. These observations reveal a plume extending from the north of Libya to the northwest of Turkey. Among simulations, the experiment assimilating IASI produces a plume whose shape is closest to the MSG observations. Nevertheless, this product does not allow conclusions to be drawn about which experiment most accurately represents the intensity of the SO_2 total columns.

Figure 10 illustrates the impact of satellite data assimilation on the simulation of volcanic SO_2 during and after the Mount Etna eruption. This plot presents the plume area and SO_2 burden computed for 3 DU and 10 DU thresholds. Observations are represented by dotted lines: OMPS (blue), IASI B (red), IASI C (purple), and TROPOMI (green). Simulated results are shown by solid lines: ref (blue), tropomi_lh_assim (green), iasi_assim (red), and joint_assim (orange).

The ref experiment consistently produces a plume area and a SO_2 burden that are weaker than those obtained when plume altitude is taken into account. For the 3 DU threshold, the plume area and the SO_2 burden increase thanks to the assimilation of TROPOMI. These metrics align well with TROPOMI and OMPS observations on 4 and 5 August, but they are underestimated compared to those derived from IASI observations, except on 4 August at 12:00 UTC and at the end of 5 August. For the 10 DU threshold, the plume area and the SO_2 burden are always close to zero. In this experiment, MOCAGE does not simulate SO_2 total columns exceeding 10 DU, whereas observations reach this threshold.

Assimilating volcanic SO_2 by taken into account the altitude of the plume increases both the plume area and SO_2 burden for both thresholds. For the 3 DU threshold, the assimilation of TROPOMI LH produces a plume area slightly higher than the ref experiment at times when TROPOMI observations are assimilated. At these times, the MOCAGE plume area is consistent with TROPOMI observations although TROPOMI LH are not available on 5 August. Following TROPOMI LH assimilation, the plume area continues to grow until 5 August at 03:00 UTC, before slowly declining. The simulated plume area remains greater than the plume areas observed by IASI B and IASI C. For the 10 DU threshold, the plume area is consistent with or

https://doi.org/10.5194/egusphere-2026-2098
Preprint. Discussion started: 8 May 2026

slightly higher than the observed plume area. The assimilation of TROPOMI LH significantly increases the SO_2 burden for both thresholds, which is consistent with observations for the 10 DU threshold. The SO_2 burden aligns well with TROPOMI observations, but the SO_2 burden values are often higher in the tropomi_lh_assim experiment compared to IASI B and C observations.

For the 3 DU threshold, the assimilation of IASI data produces a larger plume area compared to the one simulated in the tropomi_lh_assim simulation, in particular from the midpoint of the studied period. Except for the morning of 4 August, the plume area and the SO_2 burden are significantly larger than the observations. Each IASI assimilation increases both the plume area and the SO_2 burden, although the values of these metrics are already overestimated relative to the observations. For the 10 DU threshold, both the plume area and SO_2 burden are consistent with or slightly higher than the observations. Between each IASI assimilation on 4 August, the plume area and the SO_2 burden decline sharply, highlighting the rapid dissipation of the impact of assimilation between successive assimilations.

The joint assimilation of IASI and TROPOMI LH results in the largest plume area and SO_2 burden. In this simulation, the plume area and the SO_2 burden are often twice large as the observations, even for the 10 DU threshold. Nevertheless, from 5 August, the values of these metrics are consistent with the observations for the 10 DU thresholds. The overestimation of SO_2 plume area and SO_2 burden can be attributed to differences in the observed altitude between IASI and TROPOMI LH. Indeed, assimilation corrects SO_2 concentrations between two specific altitudes given by instruments, strong SO_2 concentrations may persist in the model at other altitudes, leading to an overall overestimation.

We have demonstrated that accounting for plume altitude significantly improves the overall representation of the volcanic plume in the case of Mount Etna, particularly for high total column intensities. To assess the model's accuracy in simulating SO_2 total column concentrations, a threshold-based analysis was conducted. The objective of this analysis is to evaluate the following instances:

- **Hits**: Cases where both observations and the model identify SO_2 total columns above a given threshold.
- **Misses**: Cases where observations exceed the threshold, but the model fails to detect them.
- **False alarms**: Cases where observations remain below the threshold, while the model exceeds it.

Based on these counts, two metrics are derived to quantify the model's performance.

The first metric is the probability of detection (POD), defined as the ratio between the number of hits and the sum of the number of hits and misses (Eq. 6). The POD ranges from 0 to 1. A POD score of 0 indicates that the model does not detect any of the observations exceeding the threshold. In contrast, a POD score of 1 indicates that all observations reaching a threshold are successfully detected by the model.

$$\mathrm{POD} = \frac{\mathrm{Hits}}{\mathrm{Hits} + \mathrm{Misses}} \tag{6}$$

https://doi.org/10.5194/egusphere-2026-2098
Preprint. Discussion started: 8 May 2026

The second metric is the critical success index (CSI), defined as the ratio between the number of hits and the sum of the number of hits, misses, and false alarms (Eq. 7). The CSI ranges from 0 to 1. A CSI score of 0 indicates that the model does not detect any of the observed SO_2 total columns reaching the threshold. In contrast, a CSI score of 1 signifies a perfect detection by the model of SO_2 total columns above a threshold, without misses and false alarms.

$$\mathrm{CSI} = \frac{\mathrm{Hits}}{\mathrm{Hits} + \mathrm{Misses} + \mathrm{False\ alarms}} \tag{7}$$

In the following of the paper, the notations in Table 4 are adopted. For the POD metric, times when there are neither Hits nor Misses are shown by a dot, and times when there are Misses but no Hits are shown by a cross. For the CSI metric, the dot represents the times when there are no Hits, misses, and false alarms, the cross means there are only Misses, the star shows times when there are no Hits but both Misses and False alarms are present, and the upper triangle indicates times when there are only False alarms.

	POD		CSI		
	Hits	Misses	Hits	Misses	False alarms
●	0	0	0	0	0
×	0	>0	0	>0	0
★			0	>0	>0
▲			0	0	>0

Table 4. Symbols used in plots according the studied metric and the number of hits, misses and false alarms events.

Figure 11 illustrates the probability of detection computed for three thresholds: 3 DU, 10 DU and 30 DU, compared against observations from TROPOMI, TROPOMI LH and IASI. It is important to note that, for TROPOMI LH and IASI, the POD represents the probability of detecting partial SO_2 columns between the two altitudes provided by these instruments. For TROPOMI, it is the probability of detecting a SO_2 total column exceeds a given threshold. In this figure, dots mean both Hits and Misses are null, whereas cross indicates there are only Misses.

For the 3 DU threshold, when computed against TROPOMI observations, the POD ranges between 0.8 and 0.9 in the simulation where TROPOMI data are assimilated. However, for the 10 DU and 30 DU thresholds, MOCAGE fails to detect observations reaching these thresholds. In experiments where TROPOMI observations are not assimilated, the POD computed for the 3 DU threshold is lower, dropping to 0.7 on 4 August and 0.2 on 5 August in the simulation assimilating TROPOMI LH observations. In this experiment, only observations exceeding 20 DU are assimilated, which does not represent the entire plume. The POD is particularly low on 5 August due to the absence of TROPOMI LH observations. The assimilation of IASI data results in slightly weaker PODs compared to the ref experiment for the 3 DU threshold. For the 10 DU and 30 DU thresholds, the PODs are significantly higher when the altitude of the plume is taken into account, except on 5 August in the simulation assimilating TROPOMI LH data for the 10 DU threshold. On this date, MOCAGE fails to detect SO_2 total columns

https://doi.org/10.5194/egusphere-2026-2098
Preprint. Discussion started: 8 May 2026

greater than 10 DU. The highest POD is obtained by assimilating both IASI and TROPOMI LH observations, except for the 3 DU threshold where the POD is slightly weaker than that obtained in the ref experiment.

When the POD is computed against TROPOMI LH observations, it reaches 1 in the two experiments assimilating TROPOMI LH data for the 3 DU and 10 DU thresholds. For the 30 DU threshold, a non-zero POD is obtained only in the joint_assim experiment on 4 August. For the other experiments, MOCAGE is unable to simulate SO_2 columns reaching 30 DU between the two altitudes provided by TROPOMI LH. Regarding the assimilation of IASI data alone, POD values are lower compared to the other experiments taking into account the plume altitude. This discrepancy arises because the altitude of the plume can differ between IASI and TROPOMI LH retrievals. Specifically, the SO_2 plume may be located at a higher altitude, potentially outside the altitude range covered by TROPOMI LH.

In the experiment assimilating TROPOMI data, MOCAGE is unable to detect partial columns reaching the 3 DU threshold. IASI often identifies plume altitudes above 10 km, whereas in this experiment, SO_2 concentrations are adjusted between 3 and 10 km of altitude. In both experiments where IASI observations are assimilated, POD ranges from 0.9 to 1 for the 3 DU threshold. POD value is around 0.95 on 4 August for the 10 DU threshold before dropping to approximately 0.25 on 5 August in the morning and reaches 0 in the afternoon. In these experiments, MOCAGE detects SO_2 partial columns exceeding 30 DU only on the morning of 4 August, with a POD value of around 0.4. In the afternoon, no SO_2 partial columns stronger than 30 DU are detected by MOCAGE. On 5 August, none of the observations reach 30 DU. In the experiment where only TROPOMI LH data is assimilated, the POD values are always lower than those computed in experiments assimilating IASI observations. On 4 August in the morning, POD is null because IASI observes the plume before TROPOMI. The POD values are around 0.4 on 4 August in the afternoon and around 0.1 on 5 August in the morning, dropping to 0 in the afternoon. For the 10 DU and 30 DU thresholds, the POD values are always zero or close to 0 in this experiment.

Figure 12 illustrates the probability of detection, on the first line, and the critical success index, on the second line, computed for three thresholds: 3 DU, 10 DU and 30 DU, compared against OMPS observations which are not assimilated in any experiments. The meanings of the symbols are described in Table 4.

For the 3 DU threshold, experiments that incorporate plume altitude consistently yield higher POD values. For example, on 4 August, the POD reaches approximately 0.95 in joint_assim experiment, compared to 0.7 in the ref experiment. The joint assimilation of IASI and TROPOMI LH generally produces the highest POD values. On 5 August, the experiment assimilating only TROPOMI LH data shows a lower POD, as no observations were available to constrain the model. For the 10 DU threshold, strong POD values are observed on 4 August in experiments where TROPOMI LH observations are assimilated while low POD are recorded in the other experiments. On 5 August, MOCAGE fails to simulate any SO_2 total columns exceeding 10 DU, whereas observations reach this threshold. For the 30 DU threshold, non-zero POD values are only observed on 4 August in the experiment assimilating TROPOMI LH data. In other experiments, MOCAGE underestimates the total columns, simulating values below 30 DU even when OMPS observes columns of this intensity. On 5 August, no total columns exceeding 30 DU

https://doi.org/10.5194/egusphere-2026-2098
Preprint. Discussion started: 8 May 2026

are detected by OMPS. Computed against OMPS observations, POD are improved by taking into account the plume altitude in the assimilation. This increase in POD is especially shown for the 10 DU and 30 DU thresholds.

The CSI is systematically lower than POD, when the latter is non-zero, regardless of the experiment or threshold. For the 3 DU threshold, the CSI values are consistent across the ref, tropomi_lh_assim and joint_assim experiments on 4 August, but lower when assimilating only IASI observations. On 5 August, the best CSI value is computed in the ref experiment as a large portion of the plume remains below 3 DU before TROPOMI assimilation. The assimilation of TROPOMI enables the simulation of total columns stronger than 3 DU only where TROPOMI observations are available. In experiments accounting for plume altitude, CSI values are lower due to the spread of the plume, which increases the number of false alarms. For the 10 DU threshold, non-zero CSI values are observed on 4 August, with better performance in experiments assimilating TROPOMI LH data. In the reference experiment, POD and CSI values are nearly identical, indicating few false alarms. On 5 August, the CSI drops to zero in all experiments, with symbols indicating the presence of both false alarms and misses. For the 30 DU threshold, the ratio between the POD and the CSI exceeds 2 in experiments assimilating TROPOMI LH data, suggesting that the model incorrectly detects total columns above 30 DU in some cases. On 4 August, the reference experiment shows only misses, while the iasi_assim experiment includes both misses and false alarms. On 5 August, MOCAGE incorrectly simulates total columns exceeding 30 DU in all experiments. Nevertheless, CSI values reach higher values than in the ref experiments, in particular with the 10 DU and 30 DU thresholds.

7.3 Conclusion of the case study

The eruption of Mount Etna on 4 August 2024 provided an opportunity to evaluate the impact of assimilating satellite data on the modelling of SO_2 columns and sulfate aerosols. The results highlight the importance of considering the altitude of the SO_2 plume during the assimilation process. Indeed, both the shape and intensity of the plume are more consistent with observations when plume altitude is taken into account. However, there are some discrepancies in terms of plume altitude between IASI and TROPOMI LH, which lead to differences in the plume shape simulated by MOCAGE.

8 Eruption on the Reykjanes Peninsula: 22 to 25 August 2024

8.1 Impact on SO_2 and sulfate aerosols

Figure 13 shows SO_2 during the eruption on the Reykjanes Peninsula on 23 August 2024 at 13:00 UTC, on 24 August 2024 at 10:00, 12:00, 13:00 UTC and on 25 August 2024 at 12:00 UTC. The first two rows show the analysis outputs: the assimilation of TROPOMI and the assimilation of TROPOMI LH. The assimilation of IASI and the joint assimilation are not shown because of the limited availability of observations. The last three rows display the corresponding satellite observations from TROPOMI LH, TROPOMI assuming a plume from ground level to 1 km of altitude, and OMPS assuming a plume around 3 km of altitude,

https://doi.org/10.5194/egusphere-2026-2098
Preprint. Discussion started: 8 May 2026

respectively.

The analysis outputs for 23 August 2024 at 13:00 UTC correspond to MOCAGE simulations following the first overpass of TROPOMI after the beginning of the eruption. In the ref experiment, the shape of the plume aligns well with TROPOMI observations but diverges from those of the OMPS instruments. This discrepancy arises because many TROPOMI observations are excluded from assimilation because of their low-quality flag values, which are represented in dark grey. In addition, SO_2 total columns are underestimated because in the ref experiment, observations assuming a plume at 7 km of altitude are assimilated into the model. The assimilation of TROPOMI LH produces a plume whose shape is consistent with the TROPOMI LH observations. However, the modelled plume is smaller than that observed by OMPS instrument. This is because only a small part of the plume contains SO_2 columns exceeding 20 DU, resulting in parts of the plume not being captured by the model.

On 24 August at 10:00 UTC, both the shape and intensity of the plume differ significantly between the experiments. In the ref experiment, the highest values are simulated in the west of Ireland with maximum values of about 2.5 DU. In contrast, in the experiment assimilating TROPOMI LH, the strongest values are modelled from Ireland to Scotland, reaching up to 20 DU. At 12:00 UTC, the assimilation of TROPOMI observations corrects both the shape and intensity of the plume in the ref experiment. At this time, the plume shapes in the ref experiment and in the tropomi_lh_assim experiment are consistent, despite the limited number of assimilated TROPOMI LH observations. However, the size of the plume may still be underestimated in both experiments compared to TROPOMI observations, which contain many low quality flag values. Additionally, SO_2 total columns are underestimated in the reference experiment compared to TROPOMI observations, while the simulation assimilating TROPOMI LH observations produces higher SO_2 total columns. At 13:00 UTC, in terms of intensity, the assimilation of TROPOMI LH product produces a plume that is more consistent with observations from OMPS instrument compared to the reference experiment. However, the size of the plume remains underestimated in both experiments.

On 25 August 2024 at 12:00 UTC, the ref experiment produces a plume that matches the shape observed by TROPOMI. However, in the simulation with the assimilation of the TROPOMI LH product, the part of the plume located around 65°N and between 10°W and 5°E is not modelled. Except for this region, the remaining parts of the plume are consistent with TROPOMI observations, despite the fact that most TROPOMI LH observations were assimilated on 23 August. A distinct part of the plume east of Iceland is simulated in the tropomi_lh_assim experiment but is absent in the reference experiment. Although total column values are not provided for this region, TROPOMI observations indicate the presence of data with a quality flag below 0.5. This suggests that the assimilation of TROPOMI LH may lead to a more accurate representation of the plume in this area.

Considering the plume altitude in the assimilation process has a significant impact on simulated sulfate aerosols. In the first row of the figure 14, sulfate total columns on 24 August at 18:00 UTC is shown for both ref and tropomi_lh_assim experiments. With the assimilation of the TROPOMI LH product, a region with strong sulfate aerosol total columns, up to 30 $\mu g.m^{-2}$, is modelled over the United Kingdom and extends northward to approximately 65°N. In contrast, the ref experiment shows sulfate

https://doi.org/10.5194/egusphere-2026-2098
Preprint. Discussion started: 8 May 2026

total columns of approximately 15 $\mu g.m^{-2}$. This increase in sulfate total columns leads to a slight increase in aerosol optical depth (AOD) in MOCAGE. The second row of Figure 14 presents vertical sections of sulfate concentrations at 55.1°N on 24 August at 18 UTC. With the assimilation of TROPOMI instrument, sulfate concentrations are relatively low, reaching peaks at up to 4 $\mu g.m^{-3}$ between 2 and 3 km altitude. In contrast, assimilating the TROPOMI LH product results in higher sulfate concentrations at the same location as the SO_2 plume. In this experiment, sulfate concentrations are elevated between 1 and 3 km of altitude, with a peak around 9 $\mu g.m^{-3}$. Importantly, neither the assimilation of TROPOMI nor TROPOMI LH impacts sulfate concentrations at the surface.

8.2 Comparison to independent observations

Observations from TROPOMI LH suggest that the volcanic plume is located close to the surface. When these observations are assimilated, MOCAGE simulates an increase in surface SO_2 concentrations in the same regions where the model identifies the SO_2 volcanic plume. Figure 15 presents the time series of surface SO_2 concentrations simulated by MOCAGE, in red, and observed by the AirBase network, in black, at four locations: Portlaoise in Ireland, Leeds in United Kingdom, Calais in France and Copenhaguen in Denmark. When the SO_2 plume passes over these stations, both the model and observations indicate an increase in surface SO_2 concentrations. PM10 and PM2.5 observations from the AirBase network do not show an increase in surface concentrations, as indicated by the model. Regarding AOD, it is challenging to compare its values with observations due to the presence of clouds.

To assess the model's accuracy in simulating SO_2 total column, POD against TROPOMI (assuming a plume between the ground and 1 km of altitude) and TROPOMI LH observations (a partial columns whose altitude boundaries are given by the instrument) are computed for both ref and tropomi_lh_assim experiments. The results are summarized in Table 5.

When computed against TROPOMI data, the POD reaches higher values in the ref experiment for the 3 DU threshold, except on 23 August. For the 10 DU threshold, the POD is greater values in the simulation with the assimilation of TROPOMI LH. On 25 August, MOCAGE fails to detect any observations exceeding 10 DU. On 23 August, the POD exceeds 0.90 in the tropomi_lh_assim experiment, whereas no SO_2 total columns greater than 30 DU are detected in the ref experiment. On 24 and 25 August, TROPOMI does not observe any SO_2 total columns exceeding 30 DU.

When the POD is computed against the TROPOMI LH product, MOCAGE fails to simulate partial columns reaching 3 DU between the two altitudes provided by the instrument. However, TROPOMI LH observations suggest the presence of observations stronger than 3 DU on 23 and 24 August. In the experiment assimilating TROPOMI LH data, the POD is close to 1 for the 3 and 10 DU thresholds when observations are available. For the 30 DU threshold, the POD value is 0.594 on 23 August and null on 24 August. No TROPOMI LH observations are available on 25 August. The fact that POD values computed against TROPOMI LH are null in the ref experiment, while non-null against TROPOMI, suggests an incorrect vertical location of the plume in the ref experiment. In the tropomi_lh_assim experiment, the SO_2 plume is accurately vertically represented,

https://doi.org/10.5194/egusphere-2026-2098
Preprint. Discussion started: 8 May 2026

resulting in high POD values against TROPOMI LH. Furthermore, there is a highest probability of detecting SO_2 total columns exceeding 10 DU when TROPOMI LH data are assimilated.

		TROPOMI			TROPOMI LH		
		3 DU	10 DU	30 DU	3 DU	10 DU	30 DU
ref	23/08	0.127	0.02	×	×	×	×
	24/08	0.334	0.07	●	×	×	×
	25/08	0.216	×	●	●	●	●
tropomi_lh_assim	23/08	0.472	0.612	0.905	1	0.998	0.594
	24/08	0.128	0.214	●	1	1	×
	25/08	0.152	×	●	●	●	●

Table 5. Probability of detection for the 3, 10 and, 30 DU thresholds for the ref experiments and the tropomi_lh_assim experiment. POD is computed against TROPOMI total columns assuming a plume from the ground to 1 km of altitude and TROPOMI LH partial columns. Dots represents times when both Hits and Misses are null and cross indicates time when there are only Misses.

Table 6 summarizes the POD and CSI results computed against OMPS observations. For the 3 DU threshold, the ref experiment yields higher POD values. Conversely, the tropomi_lh_assim experiment produces higher POD values for the 10 DU and 30 DU thresholds.

The small differences between POD and CSI in the ref experiment suggest a low occurrence of false alarms. In contrast, the tropomi_lh_assim experiment exhibits large differences between these two metrics, indicating a high number of false alarm events. This is particularly evident on 24 August for the 10 DU threshold and on 23 August for the 30 DU threshold. For the 3 Du threshold, better CSI values are obtained in the ref experiment, except on 23 August. For the 10 DU threshold, the CSI value is higher in the experiment assimilating the TROPOMI LH product on 23 August, while the ref experiment achieves better CSI values on 24 August. On 25 August, OMPS observations indicate the presence of total columns exceeding 10 DU which are not detected by MOCAGE. In contrast, MOCAGE simulates SO_2 total columns greater than 10 DU that are not detected by OMPS. For the 30 DU threshold, assimilating TROPOMI LH data improves the CSI metric on 23 August. On 24 August, OMPS does not detect any observations exceeding 30 DU, and MOCAGE does not model any SO_2 total columns greater than 30 DU in the reference experiment. However, MOCAGE wrongly simulates total columns greater than 30 DU when TROPOMI LH data are assimilated. On 25 August, MOCAGE wrongly detects SO_2 total columns exceeding 30 DU in both experiments.

9 Conclusions and perspectives

This study assessed the impact of explicitly considering the altitude of the volcanic plume in the assimilation of sulfur dioxide within the MOCAGE regional model covering an area stretching from Iceland to the Middle East at 0.1° of resolution. Two

https://doi.org/10.5194/egusphere-2026-2098
Preprint. Discussion started: 8 May 2026

		POD			CSI		
		3 DU	10 DU	30 DU	3 DU	10 DU	30 DU
ref	23/08	0.127	0.02	×	0.124	0.019	★
	24/08	0.334	0.071	●	0.267	0.063	●
	25/08	0.216	×	●	0.091	★	▲
tropomi_lh_assim	23/08	0.472	0.612	0.905	0.406	0.413	0.176
	24/08	0.127	0.214	●	0.101	0.025	▲
	25/08	0.153	×	●	0.053	★	▲

Table 6. Probability of detection and critical success index for the 3, 10 and, 30 DU thresholds for the ref experiments and the tropomi_lh_assim experiment. POD and CSI are computed against OMPS total columns assuming a plume around an altitude of 3 km. Symbols meaning are described in Table 4.

contrasting eruptions were analyzed: the explosive eruption of Mount Etna on 4 August 2024, characterized by a plume injected into the upper troposphere, and the effusive eruption of the Reykjanes Peninsula in August 2024, with a plume close to the surface.

In the reference configuration in which the altitude of the plume is not explicitly taken into account, the assimilation of TROPOMI total columns with a constrained injection between 3 and 10 km allows the horizontal structure of the plume to reproduce in the short term. However, when the plume is outside this vertical range, the altitude error causes a gradual deterioration of the horizontal structure during transport. In addition, injection imposed over a wide vertical range (3–10 km) leads to an artificially over-extended plume. This over-extension dilutes the maximum concentrations and distributes the SO_2 over levels subject to different wind regimes, accentuates the horizontal dispersion and increases the discrepancy with observations.

In order to ensure consistency between plume heights, a pre-processing algorithm was developed to process TROPOMI Layer Height observations prior to assimilation. This algorithm filters out non-representative altitudes, particularly at the edge of the plume. Furthermore, since IASI pixels often cover several MOCAGE grids, the total SO_2 columns and plume altitudes are interpolated in the model grid. The TROPOMI LH and IASI observations processed in this way are then assimilated, assuming that SO_2 is confined to a layer centered on the height diagnosed by the instruments. Only the SO_2 located in this layer is corrected during assimilation.

Including plume altitude information from TROPOMI Layer Height and IASI observations greatly improves the simulated vertical structure of the volcanic plume. For the Etna eruption, taking altitude into account leads to an increase in the intensity of the total columns within the plume as well as its size. In addition, there is an improvement in detection scores (POD) for high thresholds (10 and 30 DU), particularly when compared with independent OMPS observations. However, it should be noted that there are more false detections when plume altitude is taken into account during assimilation. For this case study, differences in plume altitudes are observed between IASI and TROPOMI LH, which can lead to differences in plume shape. Compared to the plume observed with MSG Ash RGB, IASI assimilation provides a better representation of the plume shape in MOCAGE.

https://doi.org/10.5194/egusphere-2026-2098
Preprint. Discussion started: 8 May 2026

In the case of the Reykjanes eruption, the assimilation of the TROPOMI Layer Height product significantly improves the vertical location of the plume and provides a better representation of the surface concentrations observed by the AirBase network. As in the previous case study, detection scores are better for high thresholds. However, false detections of high total column values occur after 24 hours of simulation.

One potential source of discrepancy lies in the assumption of a fixed plume thickness. In the present study, the same vertical thickness is prescribed for both case studies, although the actual plume thickness may vary depending on eruption intensity, atmospheric stability, and injection dynamics. An inaccurate specification of plume thickness can lead to an excessive vertical spreading of SO_2 in the model, which in turn may enhance horizontal dispersion and contribute to an overestimation of plume extent. In addition, differences in plume altitude diagnostics between instruments constitute another source of discrepancy. TROPOMI Layer Height and IASI rely on distinct spectral ranges and retrieval methodologies, which may result in different estimated plume heights for the same event. When such differences are assimilated, especially in a multi-instrument framework, they may induce corrections at multiple vertical levels and contribute to an artificial vertical broadening of the simulated plume.

Another factor that may contribute to the source of the discrepancy of the plume simulated in MOCAGE lies in the configuration of the assimilation system. In particular, the choice of horizontal and vertical correlation lengths plays a decisive role in the spatial propagation of the analysis increments. Excessive correlation lengths can lead to excessive diffusion of the assimilated signal, generating an extended plume, both horizontally and vertically. The locations where no SO_2 is detected, the information provided by TROPOMI, may be used to correct the shape plume. Similarly, the specification of the standard deviation of the background error directly influences the amplitude of the corrections made by assimilation. Too high a value can limit the impact of observations and lead to an underestimation of maximum SO_2 concentrations, while too low a value can produce excessive corrections and amplify the intensity of the simulated plume, which can produce false alarm events. Beyond assimilation issues, the uncertainties inherent in the model must also be taken into account. Chemical processes involving SO_2, particularly oxidation mechanisms and sulfate aerosol formation, introduce additional complexity that can affect the lifetime and distribution of the plume (Schumann et al., 2011). Furthermore, the meteorological fields used to force the model themselves contain uncertainties (Webster and Thomson, 2022), which may influence the representation of the transport, dispersion, and transformation of volcanic emissions.

A limitation arises in the case of multiple eruptions. During such events, several distinct layers of SO_2 may coexist at different altitudes due to successive eruptive pulses or complex injection dynamics. However, IASI and TROPOMI layer height retrievals provide only a single effective plume altitude associated with the total column. As a result, the assimilation framework assumes that the entire SO_2 column is confined to a single vertical layer, which may not reflect the true vertical structure of the plume. In particular, if multiple layers are present, the instruments may preferentially detect the highest layer, while lower-altitude plumes may remain undetectable. This can lead to incomplete vertical correction in the model and potentially bias the simulated transport, especially if the undetected lower layers are advected by different wind regimes.

Information on plume altitude from the TROPOMI Layer Height product is only available when total SO_2 columns exceed 20 DU. However, these high values generally represent only a limited fraction of the plume. In many cases, columns do not exceed this threshold, making altitude information unavailable for these eruptions. Furthermore, IASI observations are sensitive

https://doi.org/10.5194/egusphere-2026-2098
Preprint. Discussion started: 8 May 2026

to the presence of clouds and atmospheric water vapour, which complicates the detection of SO_2 plumes close to the surface. Thus, for some eruptions, no observations are available. For some eruptions, even with joint assimilation of TROPOMI LH and IASI, no SO2 plume can be modelled, although TROPOMI suggests the presence of a plume. To overcome this limitation, one approach is to set up a set of MOCAGE simulations in which the minimum and maximum injection altitudes of the plume would be perturbated. The simulated shape of the plume could then be compared with the available observations, and the member of the set with the best spatial consistency with the observations could be selected to constrain the altitude of the plume. The advantage of this approach lies in the possibility of assimilating the total SO_2 columns from TROPOMI even when they are less than 20 DU, by combining them with an estimate of the plume height.

Code availability. The code used to generate the analysis (MOCAGE and its variational assimilation suite) is research- operational code that is property of Météo-France and CERFACS and is not publicly available yet. The readers interested in obtaining parts of the code for research purposes can contact the authors of this study directly.

Data availability. All results are available upon request to the authors for 5 years.

Author contributions. MB and VG designed this study. MB carried out and interpreted the simulations. MB is the main contributor to the manuscript. VG reviewed and contributed to the manuscript.

Competing interests. The contact author has declared that none of the authors has any competing interests.

Acknowledgements. We want to thank Nicolas Theys for giving advice on the use of TROPOMI Layer Height product, Antje Inness for the explanations on the method they used to take into account the plume altitude on their assimilation process, and Olivier Coopmann for the script to determine the size of the IASI pixels.

https://doi.org/10.5194/egusphere-2026-2098
Preprint. Discussion started: 8 May 2026

References

Ashpole, I. and Washington, R.: An automated dust detection using SEVIRI: A multiyear climatology of summertime dustiness in the central and western Sahara, Journal of Geophysical Research: Atmospheres, 117, 2012.

Bacles, M., Américi, J., and Guidard, V.: Assimilation of volcanic sulfur dioxide products from IASI and TROPOMI into the chemical transport model MOCAGE: case study of the 2021 La Soufrière Saint Vincent eruption with the March 2022 version of MOCAGE, Atmospheric Measurement Techniques, 18, 2659–2680, 2025.

Bedka, K. M.: Overshooting cloud top detections using MSG SEVIRI Infrared brightness temperatures and their relationship to severe weather over Europe, Atmospheric Research, 99, 175–189, 2011.

Bouyssel, F., Berre, L., Bénichou, H., Chambon, P., Girardot, N., Guidard, V., Loo, C., Mahfouf, J.-F., Moll, P., Payan, C., and Raspaud, D.: The 2020 Global Operational NWP Data Assimilation System at Météo-France, 4, 645–664, https://doi.org/10.1007/978-3-030-77722-7_25, 2022.

Clarisse, L., Coheur, P.-F., Prata, A. J., Hurtmans, D., Razavi, A., Phulpin, T., Hadji-Lazaro, J., and Clerbaux, C.: Tracking and quantifying volcanic SO 2 with IASI, the September 2007 eruption at Jebel at Tair, Atmospheric Chemistry and Physics, 8, 7723–7734, 2008.

Clarisse, L., Clerbaux, C., Dentener, F., Hurtmans, D., and Coheur, P.: Global ammonia distribution derived from infrared satellite observations, Nat. Geosci., 2, 479–483, 2009.

Clarisse, L., Coheur, P.-F., Chefdeville, S., Lacour, J.-L., Hurtmans, D., and Clerbaux, C.: Infrared satellite observations of hydrogen sulfide in the volcanic plume of the August 2008 Kasatochi eruption, Geophysical research letters, 38, 2011.

Clarisse, L., Hurtmans, D., Clerbaux, C., Hadji-Lazaro, J., Ngadi, Y., and Coheur, P.-F.: Retrieval of sulphur dioxide from the infrared atmospheric sounding interferometer (IASI), 5, 581–594, https://doi.org/10.5194/amt-5-581-2012, publisher: Copernicus GmbH, 2012.

Clarisse, L., Coheur, P.-F., Theys, N., Hurtmans, D., and Clerbaux, C.: The 2011 Nabro eruption, a SO 2 plume height analysis using IASI measurements, Atmospheric chemistry and physics, 14, 3095–3111, 2014.

Clerbaux, C., Boynard, A., Clarisse, L., George, M., Hadji-Lazaro, J., Herbin, H., Hurtmans, D., Pommier, M., Razavi, A., Turquety, S., Wespes, C., and Coheur, P.-F.: Monitoring of atmospheric composition using the thermal infrared IASI/MetOp sounder, 9, 6041–6054, https://doi.org/10.5194/acp-9-6041-2009, publisher: Copernicus GmbH, 2009.

Coopmann, O., Guidard, V., and Vittorioso, F.: Preparation for assimilation of Meteosat Third Generation infrared sounder radiances into an atmospheric composition model for ozone and carbon monoxide forecasts, Quarterly Journal of the Royal Meteorological Society, p. e70130, 2026.

Cornut, F., El Amraoui, L., Cuesta, J., Schmisser, R., Blanc, J., and Josse, B.: Assimilation of Aerosol Observations from the Future Spaceborne Lidar Onboard the AOS Mission into the MOCAGE Chemistry: Transport Model, in: Proceedings of the 30th International Laser Radar Conference, edited by Sullivan, J. T., Leblanc, T., Tucker, S., Demoz, B., Eloranta, E., Hostetler, C., Ishii, S., Mona, L., Moshary, F., Papayannis, A., and Rupavatharam, K., pp. 645–651, Springer International Publishing, ISBN 978-3-031-37818-8, https://doi.org/10.1007/978-3-031-37818-8_83, 2023.

Courtier, P.: The ARPEGE Project at Météo-France, pp. 9–13, 1991.

Cussac, M., Marécal, V., Thouret, V., Josse, B., and Sauvage, B.: The impact of biomass burning on upper tropospheric carbon monoxide: a study using MOCAGE global model and IAGOS airborne data, 20, 9393–9417, https://doi.org/10.5194/acp-20-9393-2020, publisher: Copernicus GmbH, 2020.

https://doi.org/10.5194/egusphere-2026-2098
Preprint. Discussion started: 8 May 2026

De Wildt, M. D. R., Seiz, G., and Gruen, A.: Operational snow mapping using multitemporal Meteosat SEVIRI imagery, Remote Sensing of Environment, 109, 29–41, 2007.

El Aabaribaoune, M., Emili, E., and Guidard, V.: Estimation of the error covariance matrix for IASI radiances and its impact on the assimilation of ozone in a chemistry transport model, 14, 2841–2856, https://doi.org/10.5194/amt-14-2841-2021, publisher: Copernicus GmbH, 2021.

El Amraoui, L., Sič, B., Piacentini, A., Marécal, V., Attié, J.-L., and Frebourg, N.: Aerosol data assimilation in the chemical transport model MOCAGE during the TRAQA/ChArMEx campaign: Lidar observations, Atmospheric Measurement Techniques Discussions, 2020, 1–35, 2020.

El Amraoui, L., Plu, M., Guidard, V., Cornut, F., and Bacles, M.: A Pre-Operational System Based on the Assimilation of MODIS Aerosol Optical Depth in the MOCAGE Chemical Transport Model, 14, 1949, https://doi.org/10.3390/rs14081949, number: 8 Publisher: Multidisciplinary Digital Publishing Institute, 2022.

Emili, E., Barret, B., Massart, S., Le Flochmoen, E., Piacentini, A., El Amraoui, L., Pannekoucke, O., and Cariolle, D.: Combined assimilation of IASI and MLS observations to constrain tropospheric and stratospheric ozone in a global chemical transport model, 14, 177–198, https://doi.org/10.5194/acp-14-177-2014, publisher: Copernicus GmbH, 2014.

Feinberg, A., Sukhodolov, T., Luo, B.-P., Rozanov, E., Winkel, L. H. E., Peter, T., and Stenke, A.: Improved tropospheric and stratospheric sulfur cycle in the aerosol–chemistry–climate model SOCOL-AERv2, 12, 3863–3887, https://doi.org/10.5194/gmd-12-3863-2019, publisher: Copernicus GmbH, 2019.

Flemming, J. and Inness, A.: Volcanic sulfur dioxide plume forecasts based on UV satellite retrievals for the 2011 Grímsvötn and the 2010 Eyjafjallajökull eruption, 118, 10,172–10,189, https://doi.org/10.1002/jgrd.50753, _eprint: https://onlinelibrary.wiley.com/doi/pdf/10.1002/jgrd.50753, 2013.

George, M., Clerbaux, C., Hurtmans, D., Turquety, S., Coheur, P.-F., Pommier, M., Hadji-Lazaro, J., Edwards, D., Worden, H., Luo, M., et al.: Carbon monoxide distributions from the IASI/METOP mission: evaluation with other space-borne remote sensors, Atmospheric Chemistry and Physics, 9, 8317–8330, 2009.

Guth, J., Josse, B., Marécal, V., Joly, M., and Hamer, P.: First implementation of secondary inorganic aerosols in the MOCAGE version R2.15.0 chemistry transport model, 9, 137–160, https://doi.org/10.5194/gmd-9-137-2016, publisher: Copernicus GmbH, 2016.

Hastings, Z. W. and Sennert, S.: Report on Etna (Italy), Bulletin of the Global Volcanism Network, https://volcano.si.edu/showreport.cfm?doi=GVP.WVAR20240731-211060, accessed: 2026-01-26, 2024.

Hedelt, P., Efremenko, D. S., Loyola, D. G., Spurr, R., and Clarisse, L.: Sulfur dioxide layer height retrieval from Sentinel-5 Precursor/TROPOMI using FP_ILM, 12, 5503–5517, https://doi.org/10.5194/amt-12-5503-2019, publisher: Copernicus GmbH, 2019.

Huijnen, V., Williams, J., van Weele, M., van Noije, T., Krol, M., Dentener, F., Segers, A., Houweling, S., Peters, W., de Laat, J., Boersma, F., Bergamaschi, P., van Velthoven, P., Le Sager, P., Eskes, H., Alkemade, F., Scheele, R., Nédélec, P., and Pätz, H.-W.: The global chemistry transport model TM5: description and evaluation of the tropospheric chemistry version 3.0, 3, 445–473, https://doi.org/10.5194/gmd-3-445-2010, publisher: Copernicus GmbH, 2010.

Inness, A., Ades, M., Balis, D., Efremenko, D., Flemming, J., Hedelt, P., Koukouli, M.-E., Loyola, D., and Ribas, R.: Evaluating the assimilation of S5P/TROPOMI near real-time SO_2 columns and layer height data into the CAMS integrated forecasting system (CY47R1), based on a case study of the 2019 Raikoke eruption, 15, 971–994, https://doi.org/10.5194/gmd-15-971-2022, publisher: Copernicus GmbH, 2022.

https://doi.org/10.5194/egusphere-2026-2098
Preprint. Discussion started: 8 May 2026

Josse, B., Simon, P., and Peuch, V. H.: Radon global simulations with the multiscale chemistry and transport model MOCAGE, 56, 339–356, https://doi.org/10.3402/tellusb.v56i4.16448, publisher: Taylor & Francis _eprint: https://doi.org/10.3402/tellusb.v56i4.16448, 2004.

Kaiser, J. W., Heil, A., Andreae, M. O., Benedetti, A., Chubarova, N., Jones, L., Morcrette, J.-J., Razinger, M., Schultz, M. G., Suttie, M., and van der Werf, G. R.: Biomass burning emissions estimated with a global fire assimilation system based on observed fire radiative power, 9, 527–554, https://doi.org/10.5194/bg-9-527-2012, publisher: Copernicus GmbH, 2012.

Lamarque, J.-F., Bond, T. C., Eyring, V., Granier, C., Heil, A., Klimont, Z., Lee, D., Liousse, C., Mieville, A., Owen, B., Schultz, M. G., Shindell, D., Smith, S. J., Stehfest, E., Van Aardenne, J., Cooper, O. R., Kainuma, M., Mahowald, N., McConnell, J. R., Naik, V., Riahi, K., and van Vuuren, D. P.: Historical (1850–2000) gridded anthropogenic and biomass burning emissions of reactive gases and aerosols: methodology and application, 10, 7017–7039, https://doi.org/10.5194/acp-10-7017-2010, publisher: Copernicus GmbH, 2010.

Lamotte, C., Guth, J., Marécal, V., Cussac, M., Hamer, P. D., Theys, N., and Schneider, P.: Modeling study of the impact of SO_2 volcanic passive emissions on the tropospheric sulfur budget, 21, 11 379–11 404, https://doi.org/10.5194/acp-21-11379-2021, publisher: Copernicus GmbH, 2021.

Lefevre, F., Brasseur, G., Folkins, I., Smith, A., and Simon, P.: Chemistry of the 1991–1992 stratospheric winter: Three-dimensional model simulations, 99, 8183–8195, https://doi.org/10.1029/93JD03476, _eprint: https://onlinelibrary.wiley.com/doi/pdf/10.1029/93JD03476, 1994.

Li, C., Krotkov, N. A., Carn, S., Zhang, Y., Spurr, R. J., and Joiner, J.: New-generation NASA Aura Ozone Monitoring Instrument (OMI) volcanic SO 2 dataset: Algorithm description, initial results, and continuation with the Suomi-NPP Ozone Mapping and Profiler Suite (OMPS), Atmospheric Measurement Techniques, 10, 445–458, 2017.

Li, C., Krotkov, N. A., Joiner, J., Fioletov, V., McLinden, C., Griffin, D., Leonard, P. J. T., Carn, S., Seftor, C., and Vasilkov, A.: Version 1 NOAA-20/OMPS Nadir Mapper total column SO_2 product: continuation of NASA long-term global data record, Earth System Science Data, 16, 4291–4309, https://doi.org/10.5194/essd-16-4291-2024, 2024.

Prata, A. and Kerkmann, J.: Simultaneous retrieval of volcanic ash and SO2 using MSG-SEVIRI measurements, Geophysical Research Letters, 34, 2007.

Prata, A. J.: Satellite detection of hazardous volcanic clouds and the risk to global air traffic, 51, 303–324, https://doi.org/10.1007/s11069-008-9273-z, 2009.

Prata, F., Woodhouse, M., Huppert, H. E., Prata, A., Thordarson, T., and Carn, S.: Atmospheric processes affecting the separation of volcanic ash and SO_2 in volcanic eruptions: inferences from the May 2011 Grímsvötn eruption, 17, 10 709–10 732, https://doi.org/10.5194/acp-17-10709-2017, publisher: Copernicus GmbH, 2017.

Price, C., Penner, J., and Prather, M.: NOx from lightning: 1. Global distribution based on lightning physics, 102, 5929–5941, https://doi.org/10.1029/96JD03504, _eprint: https://onlinelibrary.wiley.com/doi/pdf/10.1029/96JD03504, 1997.

Reshi, A. R., Pichuka, S., and Tripathi, A.: Applications of sentinel-5p tropomi satellite sensor: A review, IEEE Sensors Journal, 24, 20 312–20 321, 2024.

Schmidt, A., Witham, C. S., Theys, N., Richards, N. A. D., Thordarson, T., Szpek, K., Feng, W., Hort, M. C., Woolley, A. M., Jones, A. R., Redington, A. L., Johnson, B. T., Hayward, C. L., and Carslaw, K. S.: Assessing hazards to aviation from sulfur dioxide emitted by explosive Icelandic eruptions, 119, 14,180–14,196, https://doi.org/10.1002/2014JD022070, _eprint: https://onlinelibrary.wiley.com/doi/pdf/10.1002/2014JD022070, 2014.

https://doi.org/10.5194/egusphere-2026-2098
Preprint. Discussion started: 8 May 2026

Sears, T. M., Thomas, G. E., Carboni, E., A. Smith, A. J., and Grainger, R. G.: SO2 as a possible proxy for volcanic ash in aviation hazard avoidance, 118, 5698–5709, https://doi.org/10.1002/jgrd.50505, _eprint: https://onlinelibrary.wiley.com/doi/pdf/10.1002/jgrd.50505, 2013.

Sennert, S.: Report on Reykjanes (Iceland), Bulletin of the Global Volcanism Network, https://volcano.si.edu/showreport.cfm?wvar=GVP.WVAR20240821-371020, accessed: 2026-01-26, 2024.

Sindelarova, K., Granier, C., Bouarar, I., Guenther, A., Tilmes, S., Stavrakou, T., Müller, J.-F., Kuhn, U., Stefani, P., and Knorr, W.: Global data set of biogenic VOC emissions calculated by the MEGAN model over the last 30 years, 14, 9317–9341, https://doi.org/10.5194/acp-14-9317-2014, publisher: Copernicus GmbH, 2014.

Sič, B., El Amraoui, L., Marécal, V., Josse, B., Arteta, J., Guth, J., Joly, M., and Hamer, P. D.: Modelling of primary aerosols in the chemical transport model MOCAGE: development and evaluation of aerosol physical parameterizations, 8, 381–408, https://doi.org/10.5194/gmd-8-381-2015, publisher: Copernicus GmbH, 2015.

Stockwell, W. R., Kirchner, F., Kuhn, M., and Seefeld, S.: A new mechanism for regional atmospheric chemistry modeling, 102, 25 847–25 879, https://doi.org/10.1029/97JD00849, _eprint: https://onlinelibrary.wiley.com/doi/pdf/10.1029/97JD00849, 1997.

Theys, N.: S5P/TROPOMI SO2 ATBD, Tech. rep., Tech. Rep. 1.1. 0, BIRA, available at: https://sentinels. copernicus. eu . . . , 2018.

Theys, N., De Smedt, I., Yu, H., Danckaert, T., van Gent, J., Hörmann, C., Wagner, T., Hedelt, P., Bauer, H., Romahn, F., Pedergnana, M., Loyola, D., and Van Roozendael, M.: Sulfur dioxide retrievals from TROPOMI onboard Sentinel-5 Precursor: algorithm theoretical basis, 10, 119–153, https://doi.org/10.5194/amt-10-119-2017, publisher: Copernicus GmbH, 2017.

Veefkind, J., Aben, I., McMullan, K., Förster, H., De Vries, J., Otter, G., Claas, J., Eskes, H., De Haan, J., Kleipool, Q., Van Weele, M., Hasekamp, O., Hoogeveen, R., Landgraf, J., Snel, R., Tol, P., Ingmann, P., Voors, R., Kruizinga, B., Vink, R., Visser, H., and Levelt, P.: TROPOMI on the ESA Sentinel-5 Precursor: A GMES mission for global observations of the atmospheric composition for climate, air quality and ozone layer applications, 120, 70–83, https://doi.org/10.1016/j.rse.2011.09.027, 2012.

Vittorioso, F., Guidard, V., and Fourrié, N.: Assessment of the contribution of the Meteosat Third Generation Infrared Sounder (MTG-IRS) for the characterisation of ozone over Europe, 17, 5279–5299, https://doi.org/10.5194/amt-17-5279-2024, publisher: Copernicus GmbH, 2024.

https://doi.org/10.5194/egusphere-2026-2098
Preprint. Discussion started: 8 May 2026

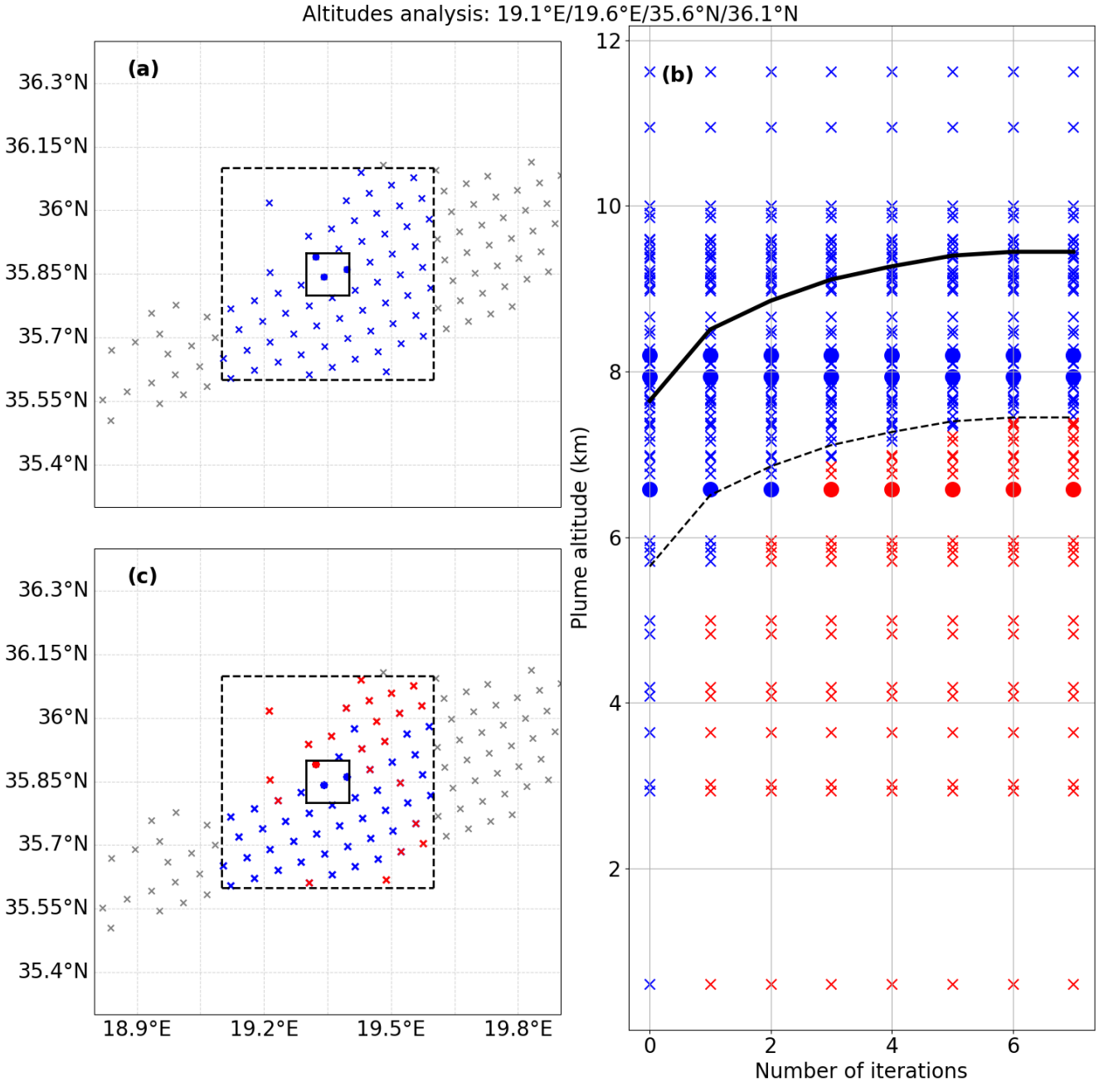

Figure 4. Example of the algorithm applied to test observation altitudes for a model meshgrid located between 35.8°N–35.9°N and 19.3°E–19.4°E delimited by the black square on figure a and c. Observations used to compute the iterative mean are shown by blue crosses or blue dots when they are in the target meshgrid. These observations are in the domain delimited by the black dotted square on figure a and c in blue. Observations which are not used are represented in grey when they are outside the domain and in red by crosses or dots when they are on the target meshgrid. The black line on figure b shows the mean altitude according to the iteration and the dotted line shows the mean altitude minus 2 km. On figure c, a new altitude equal to last computed mean altitude is assigned.

https://doi.org/10.5194/egusphere-2026-2098
Preprint. Discussion started: 8 May 2026

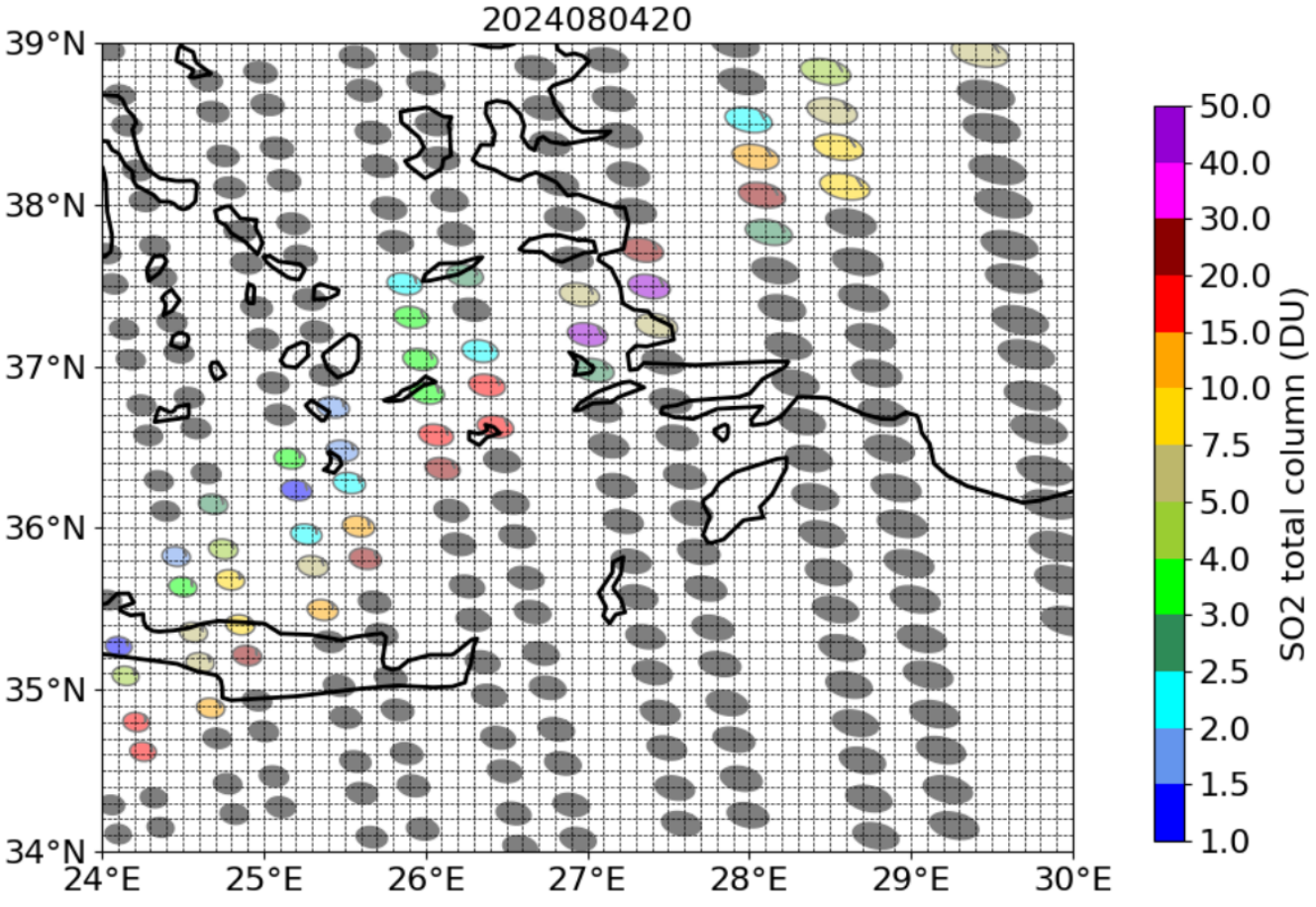

Figure 5. Footprint of IASI observations on 4 August 2024 at 20 UTC and grid of the MOCAGE regional domain. The colored ellipses represent the SO_2 total columns in Dobson Units (DU).

https://doi.org/10.5194/egusphere-2026-2098
Preprint. Discussion started: 8 May 2026

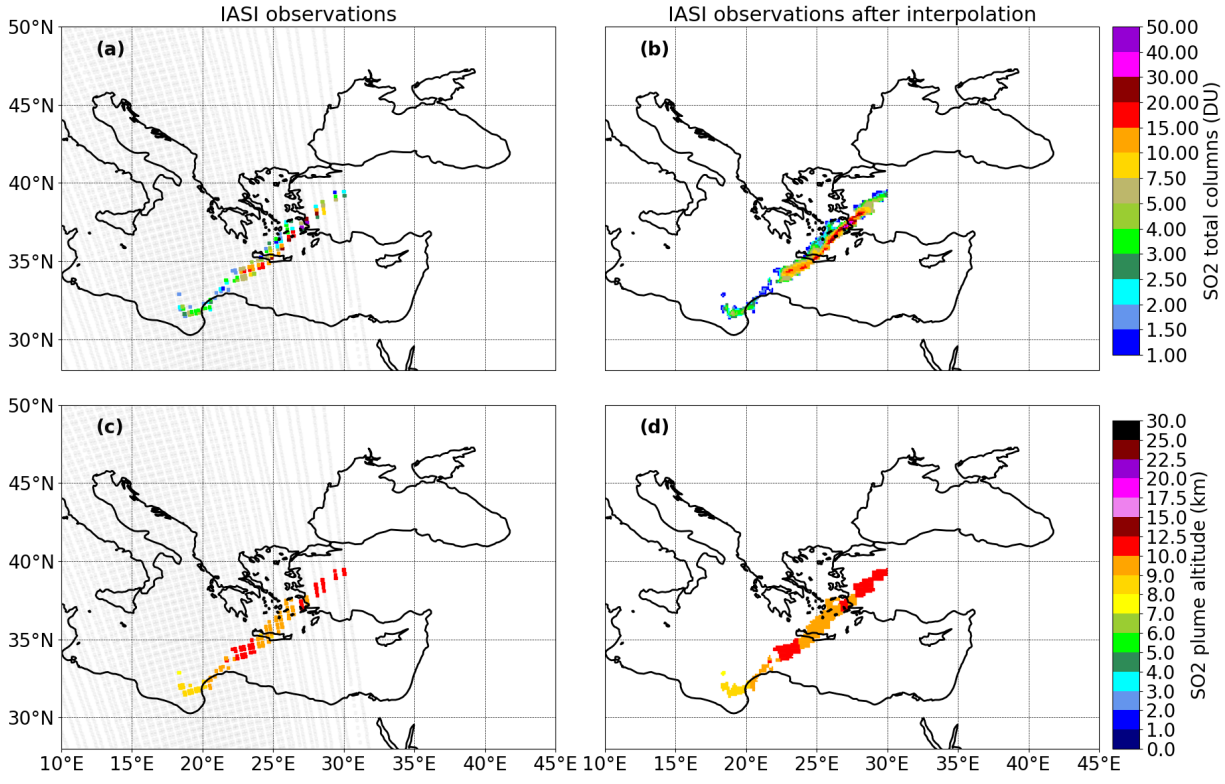

Figure 6. Observed IASI SO_2 total columns (a and b) and associated altitudes (c and d) from IASI B on 4 August 2024 at 20:00 UTC before (a and c) and after (b and d) the linear interpolation.

https://doi.org/10.5194/egusphere-2026-2098
Preprint. Discussion started: 8 May 2026

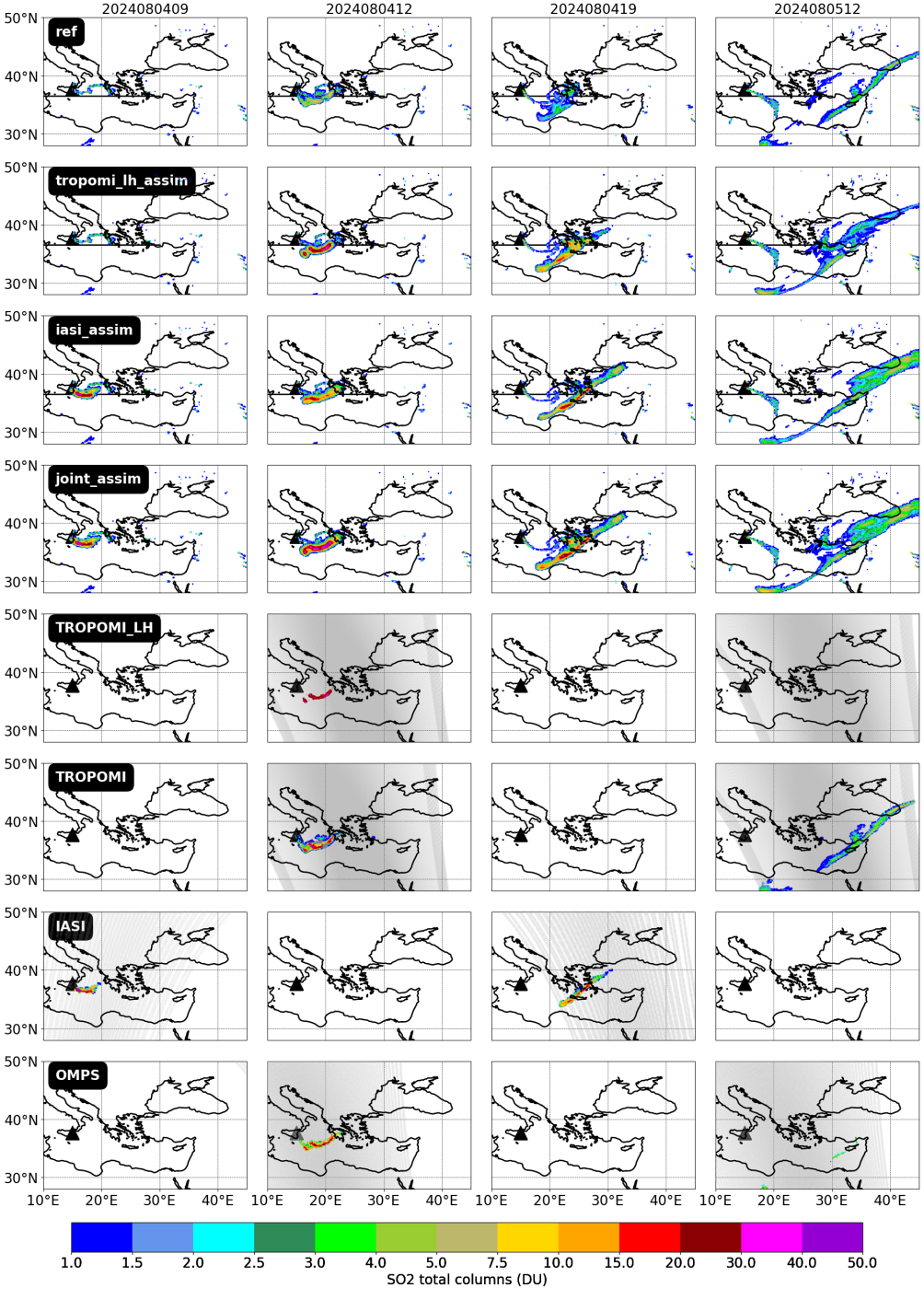

Figure 7. Observations assimilated and analyses of SO_2 total columns on 4 August 2024 at 09:00, 12:00, 19:00 UTC, and on 5 August 2024 at 12:00 UTC. The first four rows correspond respectively to the ref, tropomi_lh_assim, iasi_assim and the joint_assim analysis outputs. Observations from TROPOMI LH, TROPOMI, IASI and OMPS are plotted on the four last lines.

https://doi.org/10.5194/egusphere-2026-2098
Preprint. Discussion started: 8 May 2026

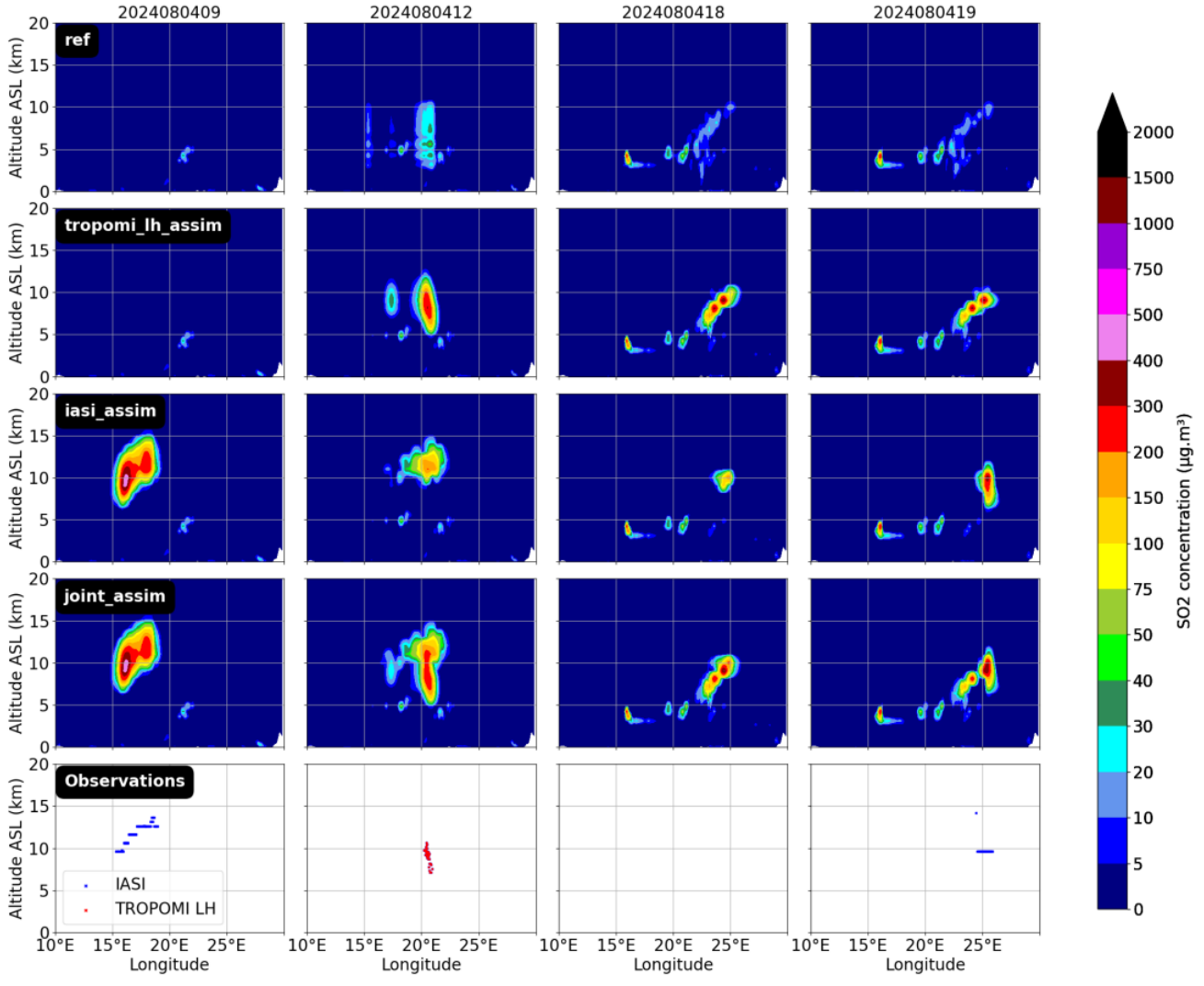

Figure 8. Vertical sections of the analysed SO_2 concentration at 36.55° N on 4 August 2024 at 09:00, 12:00, 18:00 and 19:00 UTC. Rows correspond to the TROPOMI data assimilation, TROPOMI LH data assimilation, IASI data assimilation and height of the SO_2 plume provided by the TROPOMI Layer Height product (in red) and IASI (in blue).

https://doi.org/10.5194/egusphere-2026-2098
Preprint. Discussion started: 8 May 2026

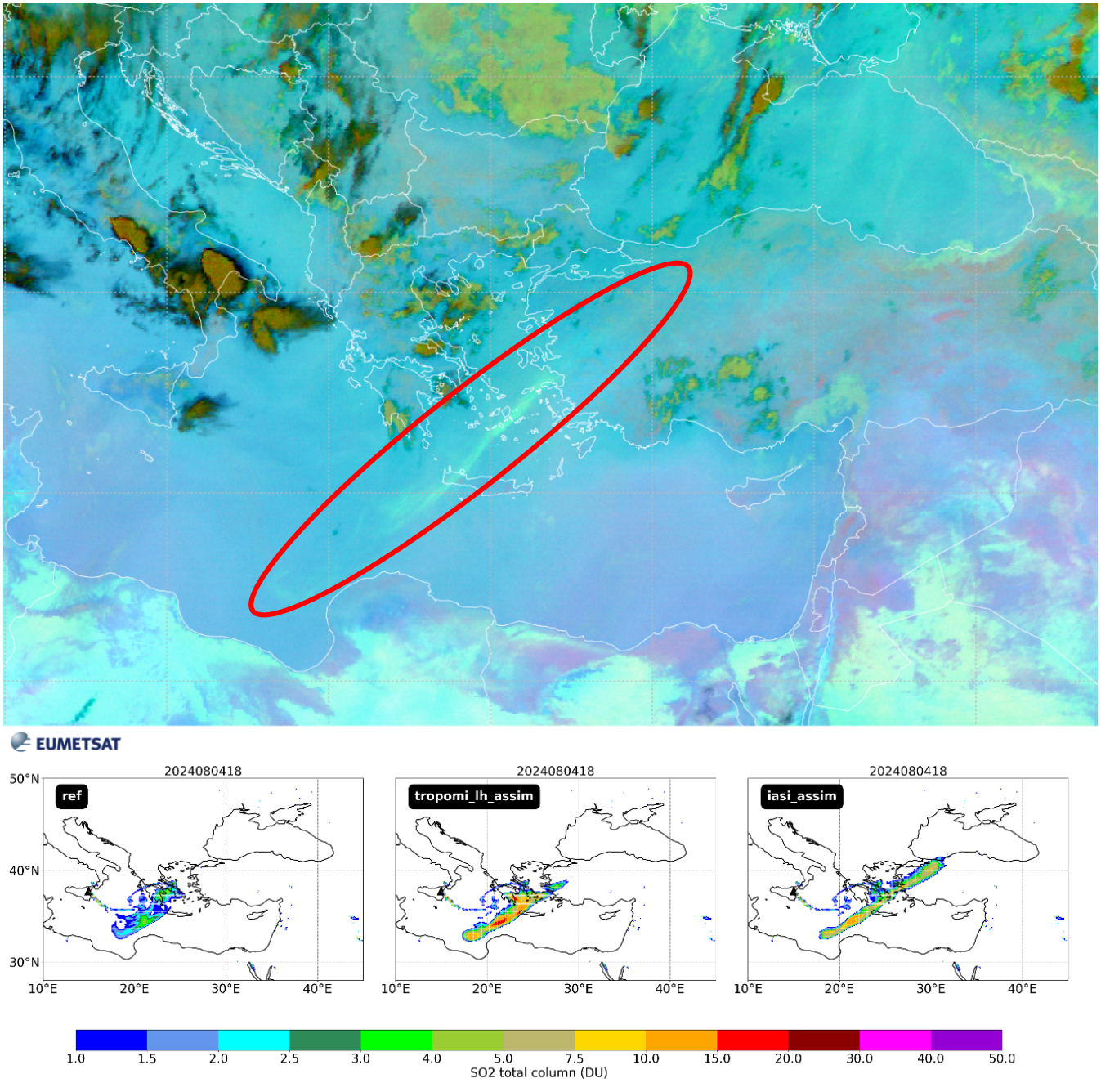

Figure 9. Ash RGB product from MSG on 4 August 2024 at 18:00 UTC at top and simulated SO_2 total columns with the assimilation of TROPOMI, TROPOMI LH and IASI.

https://doi.org/10.5194/egusphere-2026-2098
Preprint. Discussion started: 8 May 2026

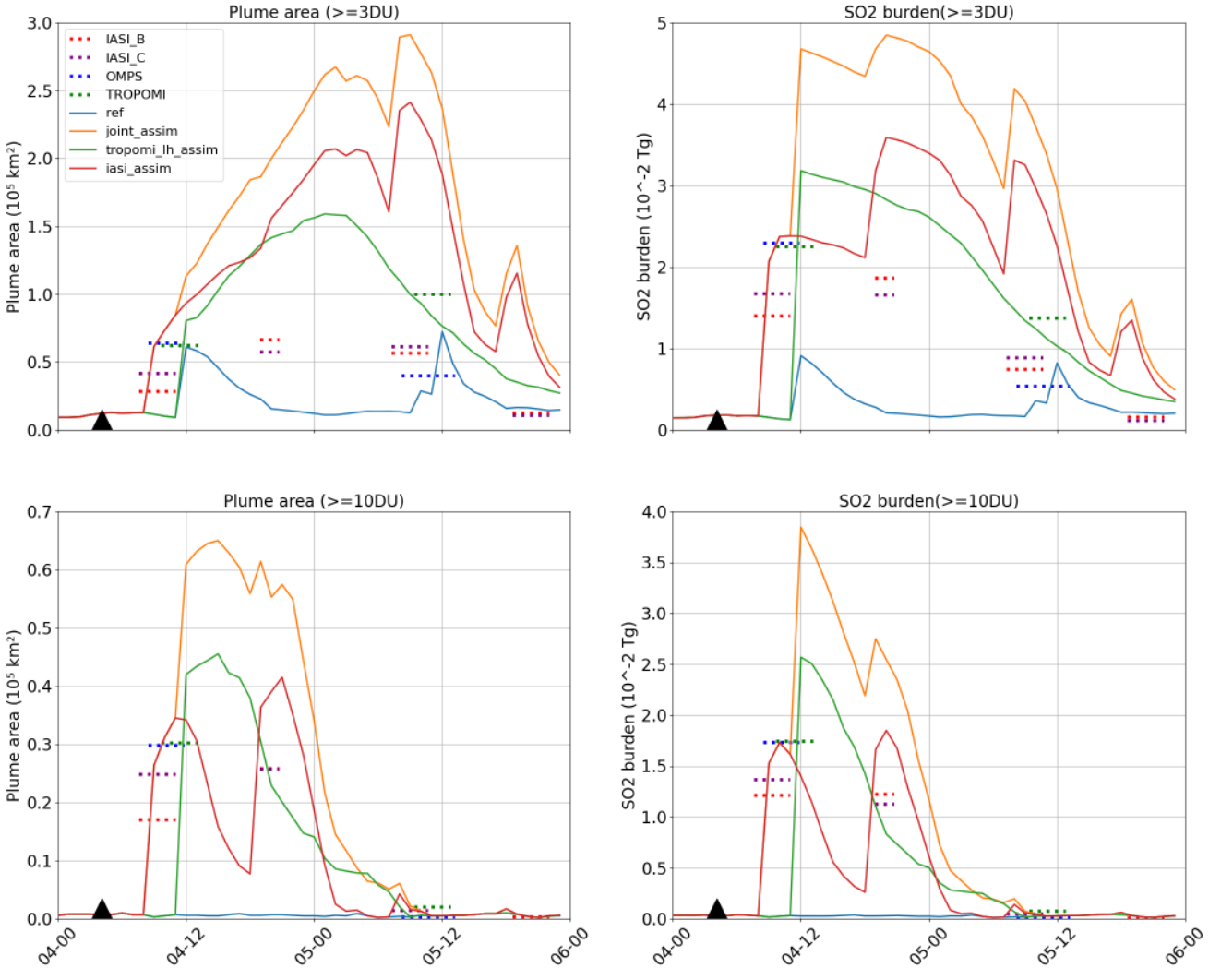

Figure 10. Temporal evolution of the SO_2 burden and plume area for thresholds of 3 and 10 DU over a sub-domain extending from 10°E to 45°E and from 28°N and 50°N after the Mount Etna eruption. Dotted lines show the observed SO_2 burden and the observed plume area by IASI B in red, IASI C in purple, OMPS in blue and TROPOMI in green. Solid lines represent the plume area and the SO_2 burden from MOCAGE for each experiments: ref in blue, iasi_assim in red, tropomi_lh_assim in green and joint_assim in orange. Black triangle represent the hour when the eruption of Mount Etna began.

https://doi.org/10.5194/egusphere-2026-2098
Preprint. Discussion started: 8 May 2026

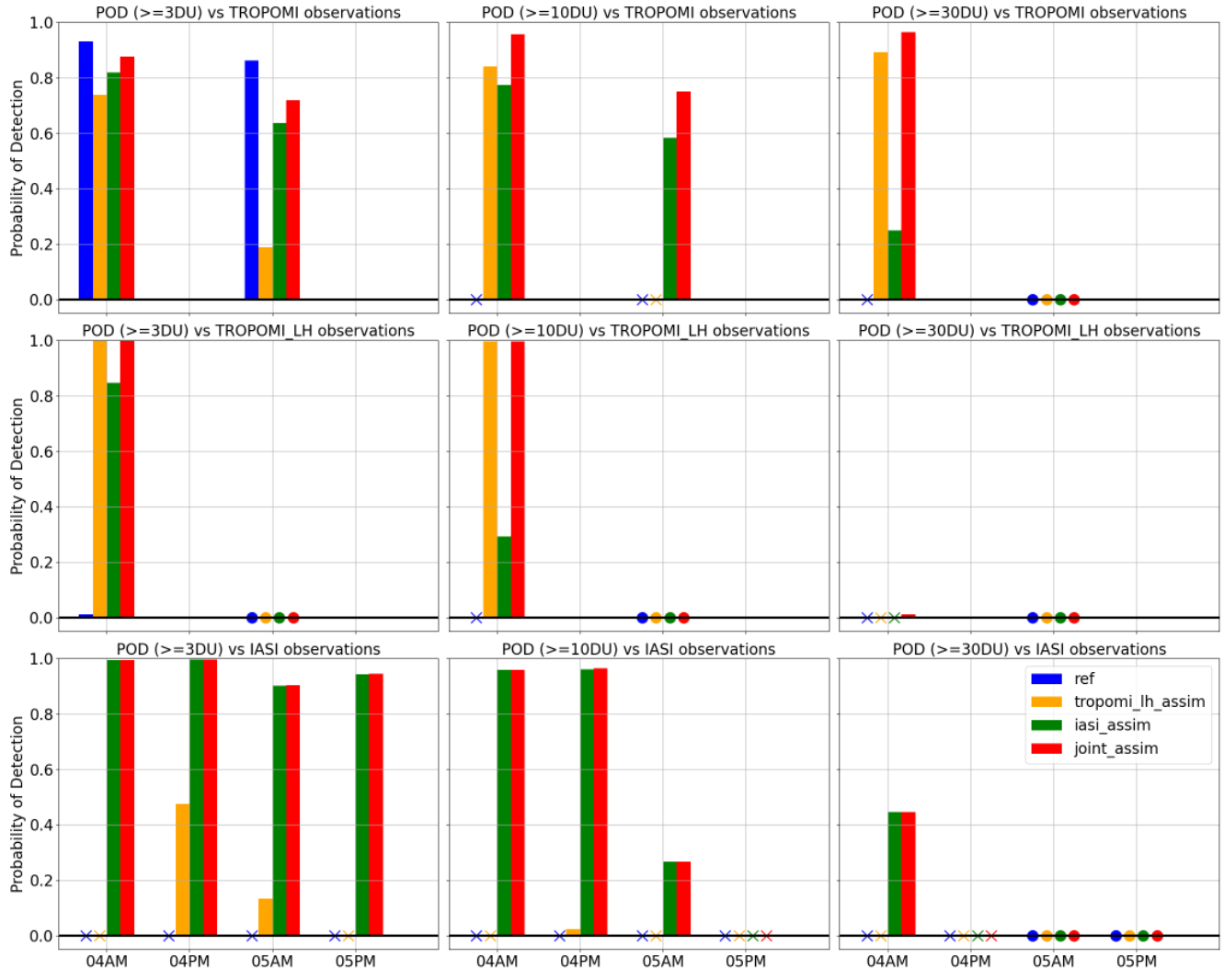

Figure 11. Probability of detection for the 3, 10 and, 30 DU thresholds for the four experiments: ref in blue, tropomi_lh_assim in orange, iasi_assim in green and, joint_assim in red. POD is computed against TROPOMI (first row), TROPOMI LH (second row) and IASI observations (last row). Dots represents times when both Hits and Misses are null and cross indicates time when there are only Misses. AM: morning, PM: afternoon.

https://doi.org/10.5194/egusphere-2026-2098
Preprint. Discussion started: 8 May 2026

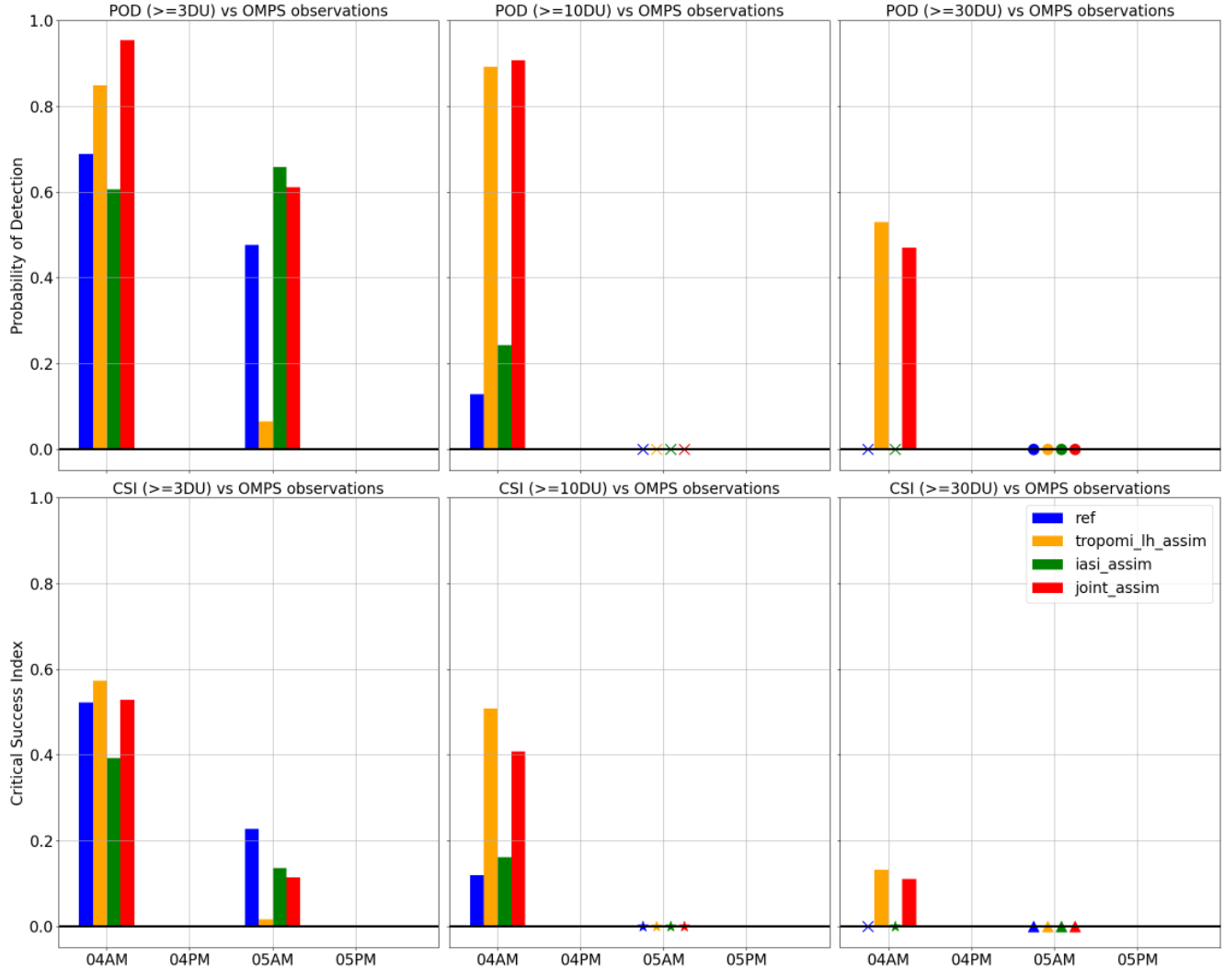

Figure 12. Probability of detection (first row) and critical success index (second row) for the 3, 10 and, 30 DU thresholds for the four experiments: ref in blue, tropomi_lh_assim in orange, iasi_assim in green and, joint_assim in red. POD and CSI are computed against OMPS observations (last row). The meaning of the symbols is described in Table 4.

https://doi.org/10.5194/egusphere-2026-2098
Preprint. Discussion started: 8 May 2026

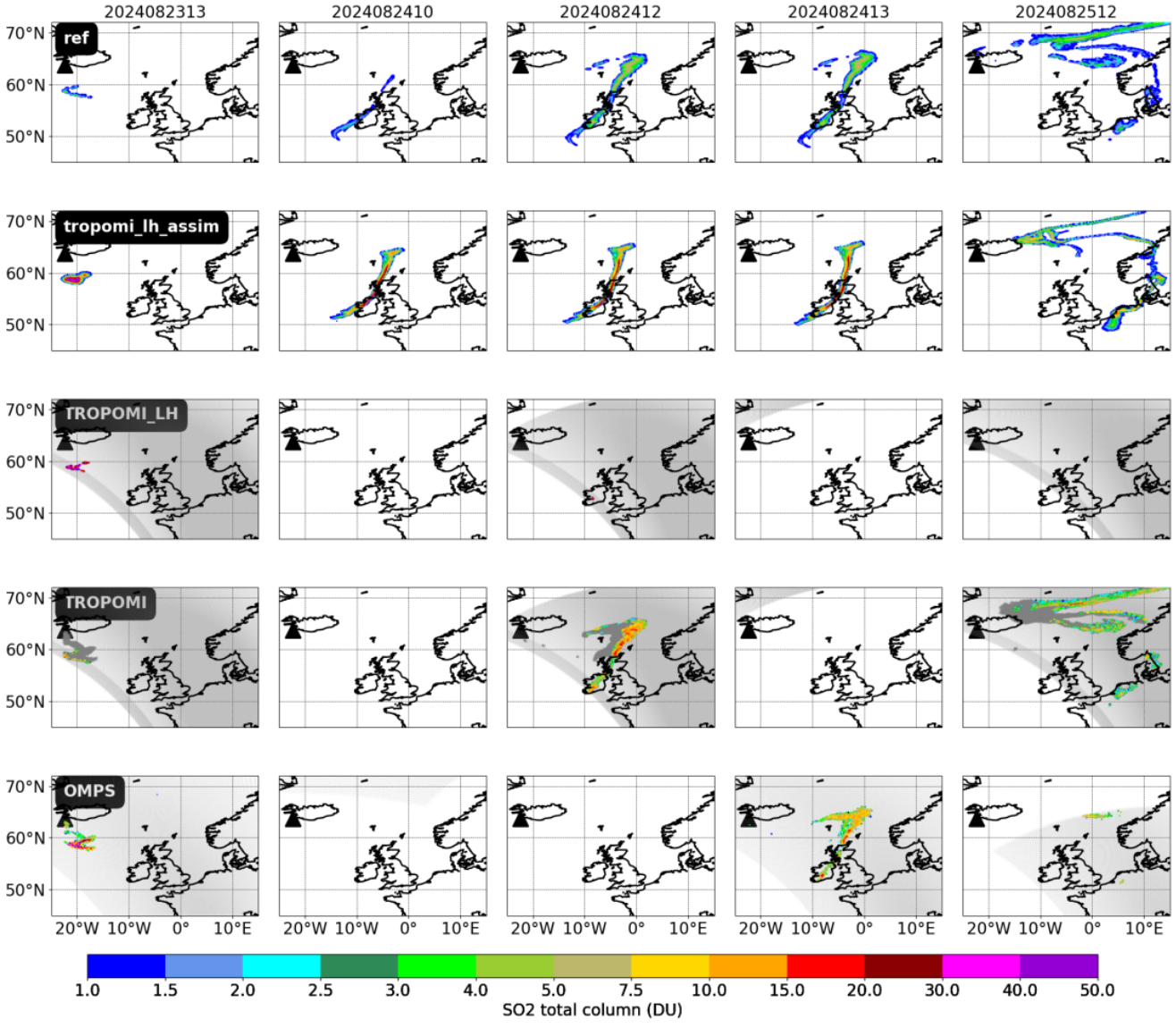

Figure 13. Analyses of SO_2 total columns on 23 August 2024 at 13:00, on 24 August 2024 at 10:00, 13:00, and on 25 August 2024 at 13:00 . The first two rows correspond respectively to the ref and tropomi_lh_assim analysis outputs. Observations from TROPOMI LH, TROPOMI and OMPS are plotted on the three last lines. Overpasses of satellites are plotted in light grey. For TROPOMI observations, data points in dark grey represent observations with a quality flag below 0.5.

https://doi.org/10.5194/egusphere-2026-2098
Preprint. Discussion started: 8 May 2026

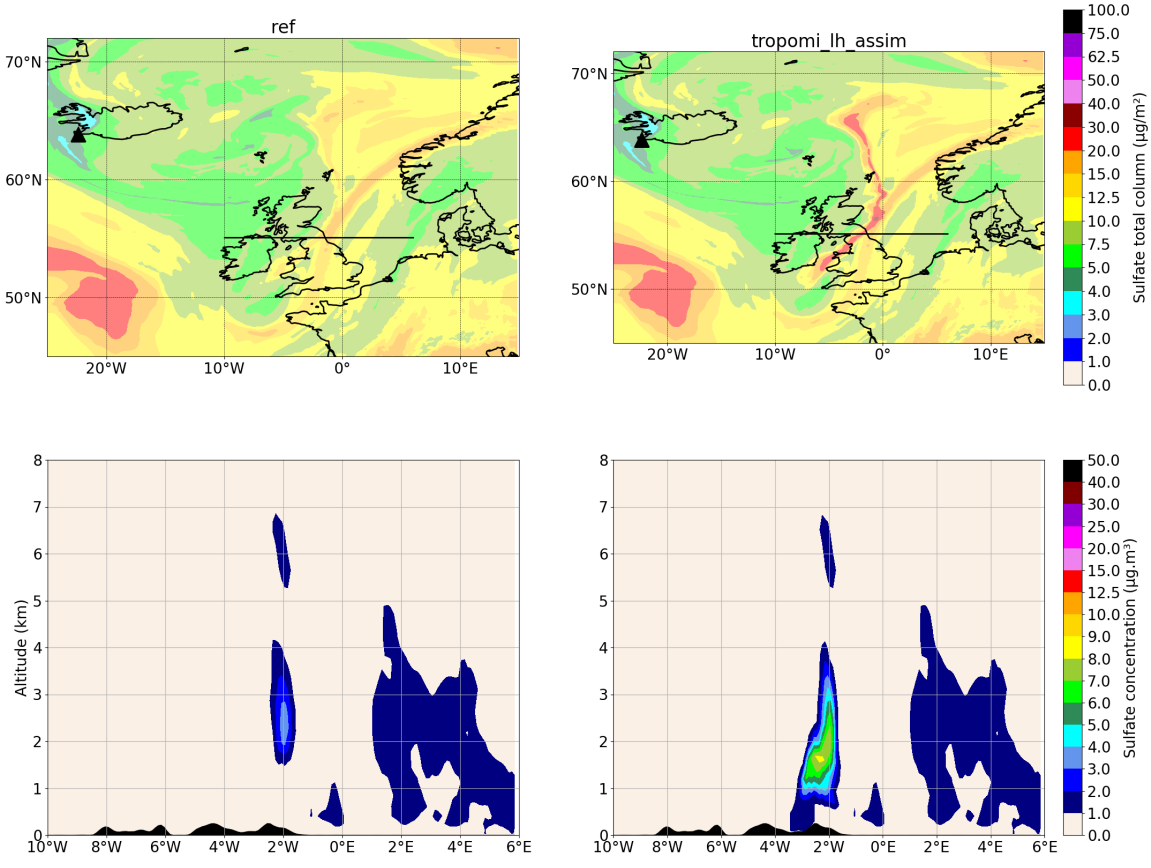

Figure 14. Sulfate aerosols total columns in the ref and tropomi_lh_assim experiments on 24 August at 18 UTC on the first row. The second row shows vertical sections of sulfate concentrations at 55.1°N on 24 August at 18 UTC.

https://doi.org/10.5194/egusphere-2026-2098
Preprint. Discussion started: 8 May 2026

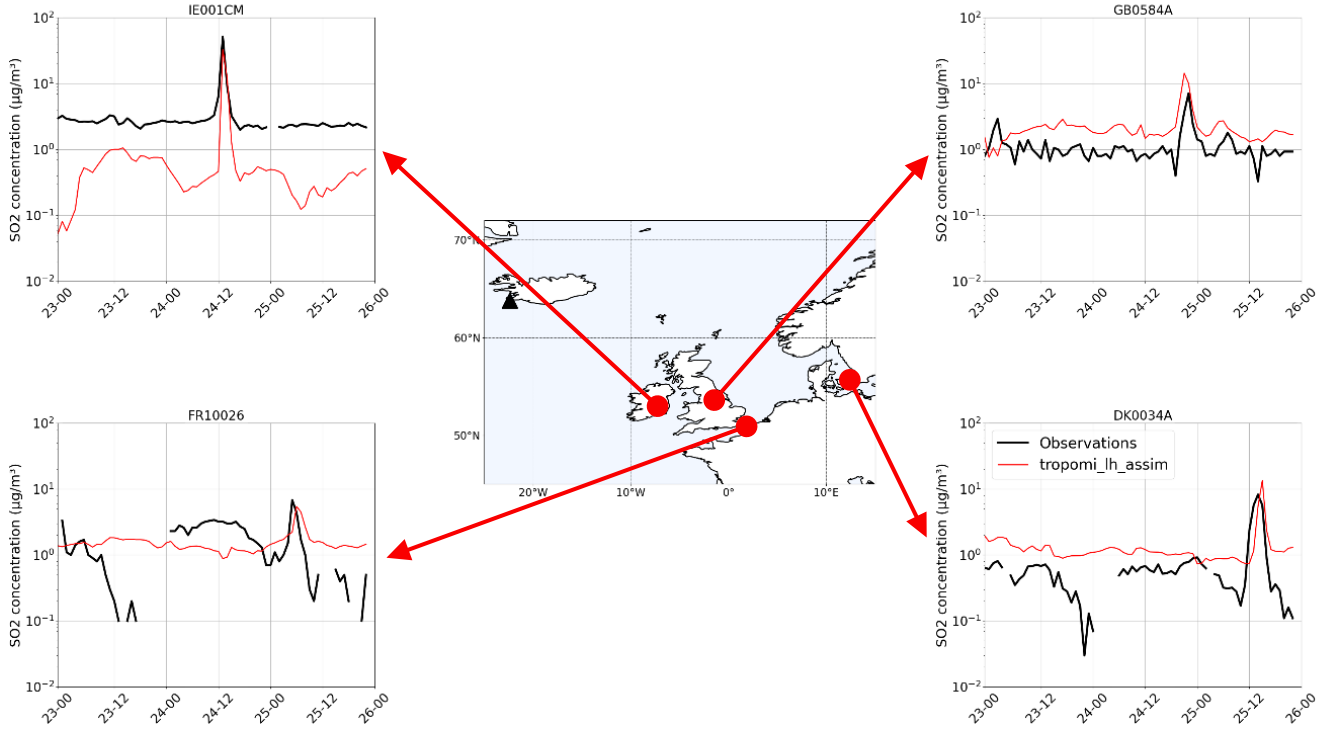

Figure 15. Surface SO_2 concentrations observed (in black) and modelled by assimilating TROPOMI LH with a horizontal correlation of 0.25° (in green), 0.1° (in red) and by assimilating TROPOMI (in purple). Timeseries are plotted for 24 and 25 August 2024 in Portlaoise (Ireland), in Leeds (United Kingdom), in Calais (France) and in Copenhaguen (Denmark).